CHAPTER IV

RESULTS AND DISSCUSION

In this study, poly(AM-*co*-IA)/mica superabsorbent nanocomposites were prepared by free radical polymerization in aqueous solutions of AM, IA and the crosslinker N-MBA.When the suspension of mica was mixed with monomer solution for 2 h for intercalation. The N-MBA crosslinker, APS initiator and TEMED co-initiator were then added and the mixture was purged with nitrogen gas to replace the oxygen in the system. In the polymerization process, first step is a reaction between APS and TEMED in which the TEMED molecule is left with an unpaired valence electron as shown in Scheme 1 (28). The activated TEMED molecule can combine with an AM and anionic comonomer such as IA and N-MBA crosslinker molecules. In the process, the unpaired electron is transferred to the monomeric units, so that they in turn become reactive. Another monomer or comonomer can therefore be attached and activated in the same way. The polymer (AM) or copolymer (AM/IA) can continue growing indefinitely, with the active center being continually shifted to free ends of the chain. Crosslinker molecules can incorporate into chains simultaneously and forming a permanent link between them. The process of both polymerization and crosslinking has been taken place for half an hour for the reaction to reach the highest conversion, which yields a semi-viscous solution (29).

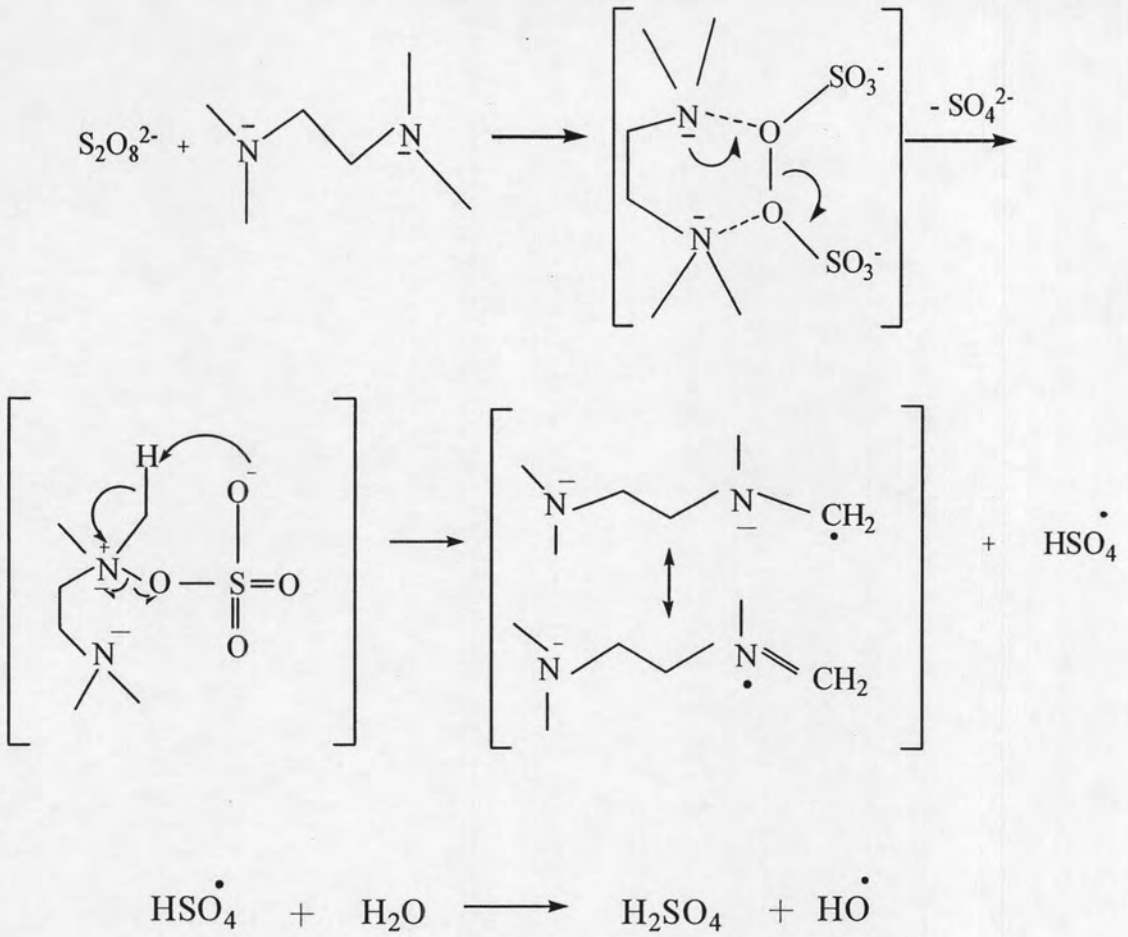

$$HSO_4^{\bullet} + H_2O \longrightarrow H_2SO_4 + HO^{\bullet}$$

Scheme 1 Formation of radicals from peroxodisulfate and TEMED

4.1 Effects of Influential Parameters on Absorbency of Poly(AM-*co*-IA) Copolymer

4.1.1 Effect of Itaconic Acid Concentration

4.1.1.1 Effect of Itaconic Acid Concentration on Water Absorbency

The effect of IA concentrations on the water absorbency of poly(AM-*co*-IA) copolymers is shown in Table 4.1 and Figure 4.1.

Table 4.1 Effect of itaconic acid concentration on water absorbency (Q) of the synthesized copolymers*

Itaconic acid (mole percent)	Water absorbency (Q) (g g^{-1})
0	35±1
1	372±9
2	383±14
3	394±9
4	476±6
5	640±7
6	ND

*Polymerization reactions were carried out at 0.2% mole of N-MBA, 0.3% mole of APS, 1.2% mole of TEMED, 50°C, and 30min, ND = Not detected.

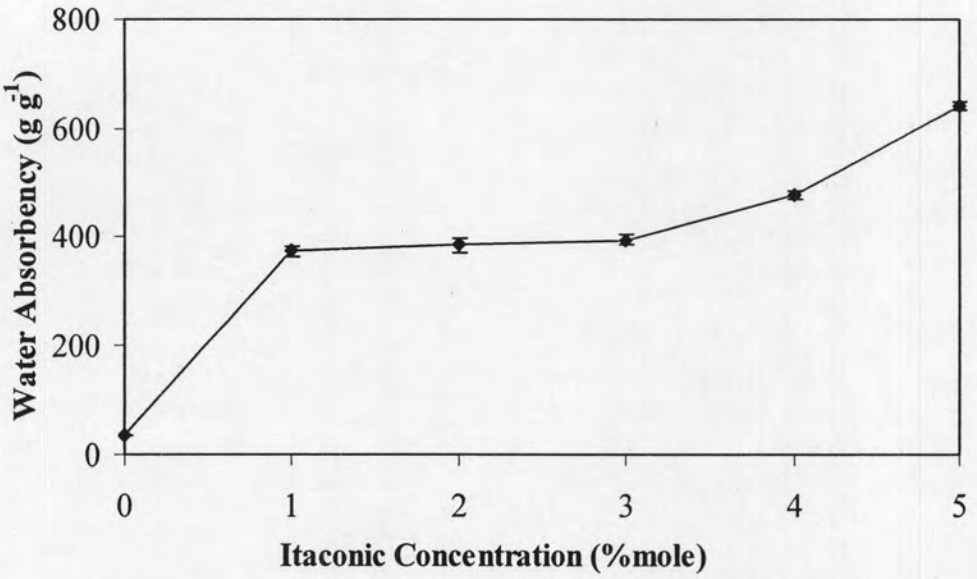

Figure 4.1 Effect of itaconic acid concentration (%mole) on the water absorbency (Q) of poly(AM-*co*-IA) copolymer at 0.2% mole of N-MBA, 0.3% mole of APS, 1.2% mole of TEMED , 50°C, and 30min.

The values of water absorbency of polyacrylamide (PAM) is only at 35±1 times its dry weight, but the values of water absorbency of poly(AM-*co*-IA) copolymer vary from 372±9 to 640±7 times its dry weight, which are 10-20 times larger. At 5% mole IA, the highest water absorbency value at 640±7 times its dry weight was achieved. The reaction was limited at 5% mole of IA due to the fact that the gel was not formed above such concentration for over an hour. Above 5% mole of IA, a slurry was formed which could not be applied as superabsorbent polymers in personal care applications. Moreover, the product cannot be dewatered with methanol and the gel could not be obtained. Pulat and Eksi (30) reported that increasing the amount of IA in copolymeric structure decreases the effective crosslinking densities of polymer networks. As IA could not form any hydrogel by itself, the presence of an excessive amount of IA in the monomer mixture made the system more difficult to form gel (30). The degree of swelling of synthesized copolymers of acrylamide (AM) and itaconic acid (IA) mainly depends on repulsive forces between the hydrophilic pendants (amide and carboxylic groups) in their structures. The reactivity ratios of AM and IA are 0.77 and 1.36, respectively (31) *i.e.* itaconic acid monomer molecules are used up earlier than acrylamide monomer if the monomer feed concentrations are equal. Therefore, the structure of the copolymer contains more AM units than IA units owing to a higher acrylamide concentration. The addition of itaconic acid into the the polymer network with increasing IA concentration will simultaneously enhances the presence of the carboxyl groups (-COOH), resulting in an increase in electrostatic repulsive force between charge sites on carboxylate ions upon their complete dissociation (22); thus the network is expanded. The expanded structure with high IA content causes a high swelling of the hydrogel.

4.1.1.2 Effect of Itaconic Acid Concentration on Absorbency Under Load (AUL)

The water absorbency under load (0.28 psi and 0.70 psi) of the poly(AM-*co*-IA) copolymer, synthesized by various concentrations of IA (% mole) with 0.2% mole of N-MBA, 0.3% mole of APS and 1.2% mole of TEMED is shown in Table 4.2 and Figure 4.2.

Table 4.2 Effect of itaconic acid concentration on water absorbency under load (AUL) of the synthesized copolymers*

Itaconic acid concentration (%mole)	absorbency under load (AUL) ($g\ g^{-1}$)	
	0.28 psi.	0.7 psi.
1	8.88±0.49	8.21±0.6
2	9.6±1.04	7.24±1.44
3	10.54±0.37	8.86±1.3
4	10.6±0.11	9.17±0.88
5	10.42±0.21	7.54±1.25

*Polymerization was carried out at various IA concentrations, 0.2% mole of N-MBA, 0.3% mole of APS, 1.2% mole of TEMED, 50°C, and 30 min.

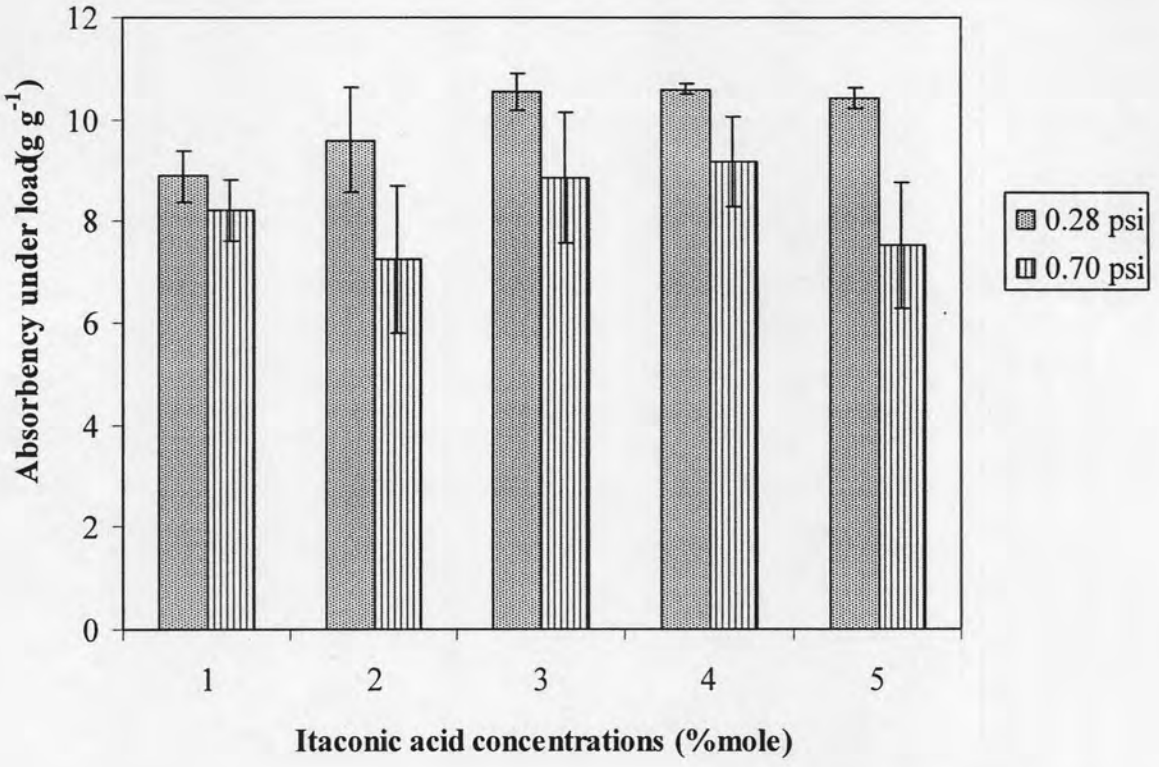

Figure 4.2 Effect of itaconic acid concentration (%mole) on the absorbency under load of the poly(AM-*co*-IA) copolymer at 0.2% mole of N-MBA, 0.3% mole of APS, 1.2% mole of TEMED, 50°C and 30min.

The highest AUL of 0.28 psi. was found at 3% mole of IA, which gave a value of 10.54 g g^{-1}. Likewise, the highest AUL of 0.70 psi was found at 4% mole of IA, which gave a value of 9.17 g g^{-1}. It is well known that the gel strength of hydrogel was in the inverse ratio of equilibrium swelling ratio (32). The tendency of absorbency under load increased with increasing the concentration of IA, suggesting a strong repulsion between negative charges of the carboxylate anions in the network.

4.1.1.3 Effect of Itaconic Acid Concentration on Viscoelastic Properties of Poly(AM-*co*-IA) Copolymer

The plot of G'(γ) and G''(γ) of poly(AM-*co*-IA) at various IA concentrations is given in Figure 4.3.

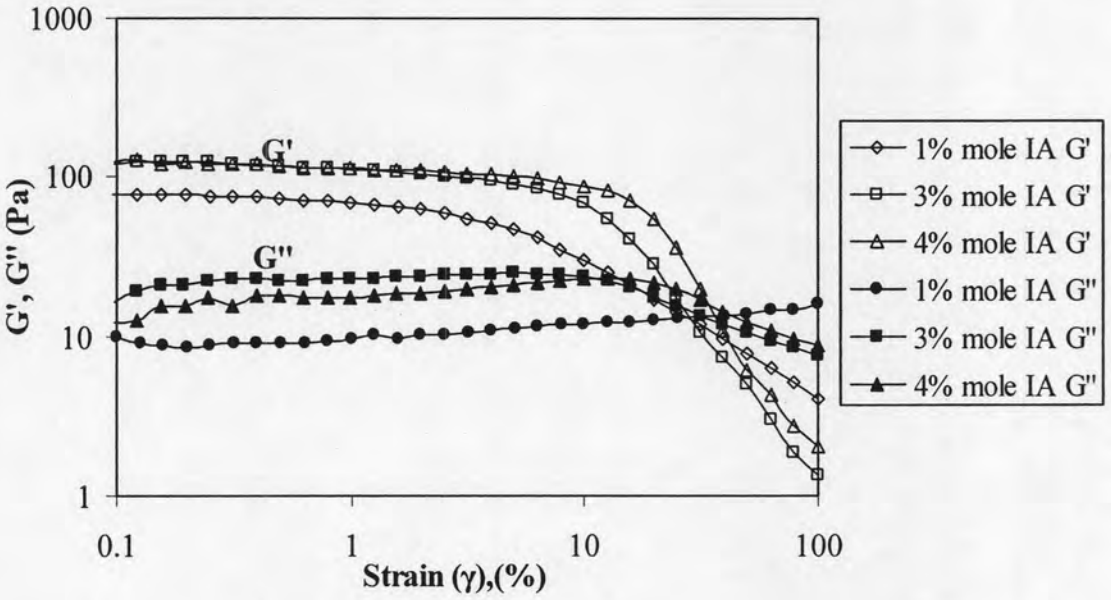

Figure 4.3 Strain dependence of the G' and G'' at the constant angular frequency (1 rad/s) for the synthesized poly(AM-*co*-IA) copolymer at various IA concentrations, 0.2% mole of N-MBA, 0.3% mole of APS, 1.2% mole of TEMED, 50°C, and 30min.

The effect of shear strain on the measured G' and G'' at the constant frequency (ω = 1rad/s) was evaluated. As expected, the G' is always higher than the G''. Below 1% deformation, it was observed that G'(ω) is independent on the applied strain, indicating the linear viscoelastic (LVE) behavior (17). As a result, the frequency sweep test was carried out between 0.1 and 100 rad/s as shown in Figure 4.4.

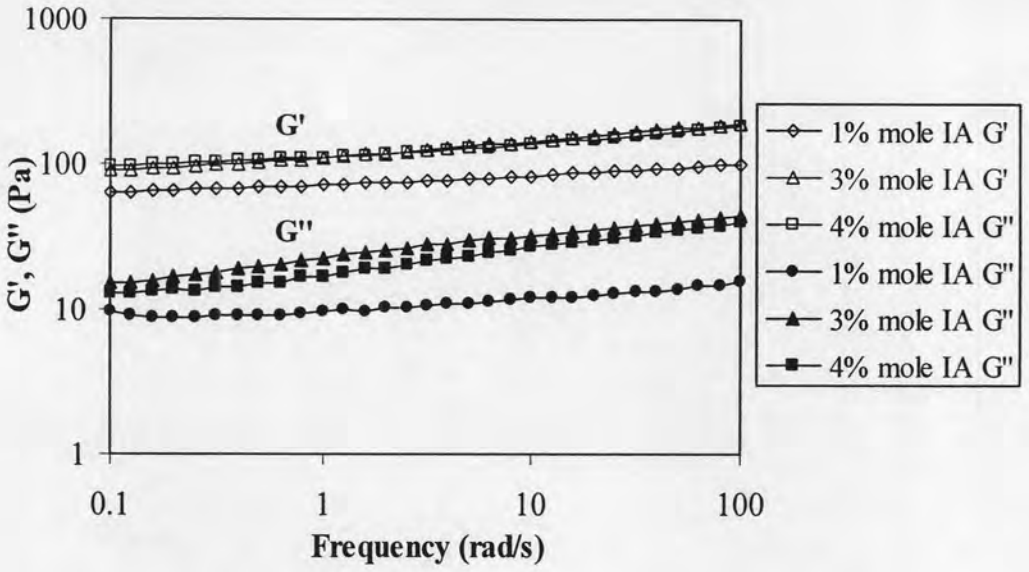

Figure 4.4 Angular frequency dependence of G' and G'' at the constant strain for the synthesized poly(AM-*co*-IA) copolymer at various IA concentrations, 0.3% mole of APS, 0.2% mole of N-MBA, 1.2% mole of TEMED, 50°C, and 30min.

For viscoelastic properties of the hydrogels prepared with different IA concentrations, G'(ω) of the copolymers prepared with different concentrations of IA are always higher than those of G'' (ω) over the whole frequency range, as shown in Figure 4.4. It is clear that the storage modulus (G') of the copolymers shows almost no dependence on the frequency. These features are characteristics of a "strong gel" (stable viscous liquid) (33). The elastic behavior of the polymeric gel predominates over its viscous behavior, and the swollen gel also exhibits the mechanical rigidity. The fact that G'>>0 reflects a substantial presence of the existence of a network structure, composed of the crosslinked polymer (34). The impressive strength (or "gel strength") of these swollen samples was indicated by the magnitudes of G'(ω) of the gel instead of coming from water, which is the majority component in the gel. The reason is that G' of water is a very low number, which is approximately at zero (as

much as the value of G' for the majority component (water) is G'= 0). As mentioned above, when G'>>0 reflects a substantial presence of the existence of a network structure. This indicates that increase in the IA concentration results in the increase of G', which is corresponding to the gel strength. In contrast, Karadag et al. (18) reported that the crosslink density decreased with increasing IA concentration in the hydrogels, which was correlated to the elastic state. For our present research, we found that the gel strength increased somewhat with increasing IA concentration until constant at 3% mole. Further increase in IA concentration did not increase the G' value. The G' value are increased from 1% to 3% mole IA; they are 63 and 96 Pa (at 0.1% strain), respectively. The increment of G' from 1% mole of IA is approximately at 52%. These results suggested the gel strength improvement which could be explained by a strong repulsion between negative charges of the carboxylate anions in the network, and such results correlated well with the water absorbency under load (as seen in Section 4.1.1.2).

4.1.2 Effect of *N,N'*-methylenebisacrylamide Concentration on Water Absorbency

The water absorbency of the superabsorbent polymers, synthesized by 1, 3 and 5 mole percent of AM/IA with 0.3% mole of APS, 1.2% mole of TEMED and various concentrations of the N-MBA crosslinker is shown in Table 4.3 and Figure 4.5.

Table 4.3 Effect of crosslinker concentration (mole percent) on water absorbency (Q) of the synthesized copolymers*

Concentration of N-MBA (%mole)	Water absorbency (Q) (g g^{-1})		
	AM/IA: 99/1	AM/IA: 97/3	AM/IA : 95/5
0.2	372±9	394±9	640±7
0.5	112±2	208±5	313±10
0.7	86±3	145±14	202±3
0.9	69±4	118±4	135±2

*Polymerization was carried out at 0.3% mole of APS, 1.2% mole of TEMED, 50°C, and 30 min.

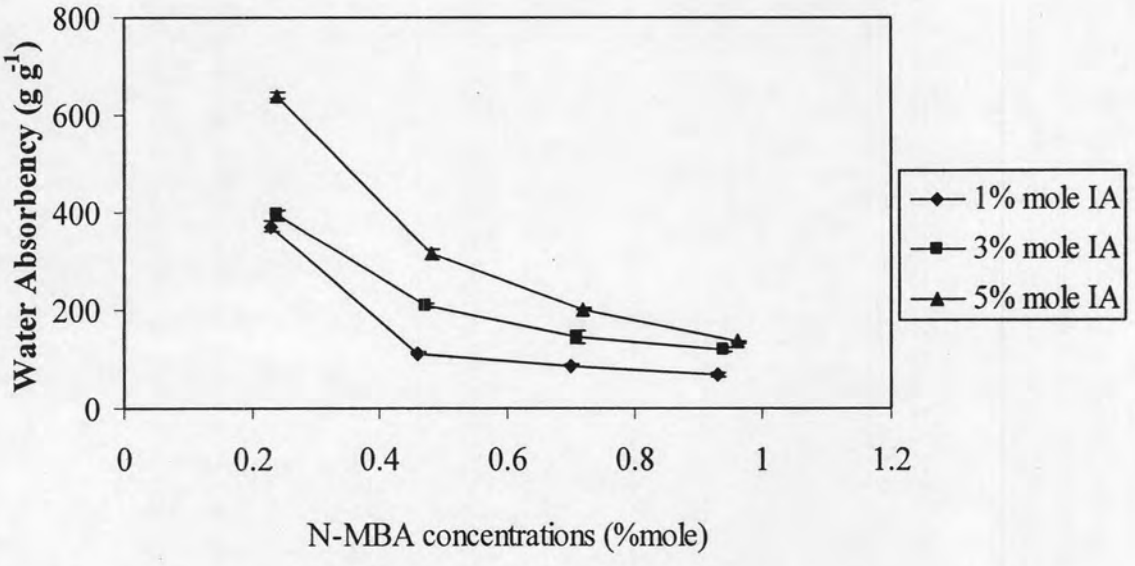

Figure 4.5 Effect of crosslinker concentration on the water absorbency (Q) of the synthesized poly(AM-*co*-IA) copolymer at various IA concentrations with 0.3% mole of APS, 1.2% mole of TEMED, 50°C and 30min.

The relationship between water absorbency and crosslinker concentration is illustrated in Figure 4.5. When the crosslinker concentration increases, the chemical crosslinking density of the synthesized copolymers also increases. This could result in a decrease in the space between the copolymer chains leading to a decrease in water absorbency. Apart from modifying the swelling and mechanical properties, the crosslinker affects and controls the amount of soluble polymer formed during the polymerization (35).

On the other hand, the relationship between the absorbency and network structure parameters was investigated by Flory and given as the following equation (20):

$$q_m^{5/3} \cong \frac{\left[\frac{1}{2}\frac{i}{v_u}\frac{1}{S^{*1/2}}\right]^2 + \left[\frac{1}{2} - \chi\right]/V_1}{v_e/V_0} \qquad (2.1)$$

where q_m is the equilibrium swelling ratio, v_e/V_0 is the number of effectively crosslinked chains in a unit volume, S^* is the ionic strength of the swollen liquid, i/v_u is the concentration of fixed charge referred to the unswollen networks, χ is the polymer-solvent thermodynamic interaction parameter, and V_1 are the molar volume of water. S^*, i/v_u, χ and V_1 are constant when the absorbed liquid is fixed. Therefore, v_e/V_0 is the only factor that can influence the absorbency. The factor v_e/V_0 in the Equation (2.1) expresses the crosslink density and inverse effect on the absorbency. Therefore, the increasing N-MBA crosslinker concentration can result in a decrease in absorbency.

4.1.3 Effect of the Polymerization Temperature on Water Absorbency

The water absorbency of the copolymers synthesized by crosslinking polymerization at various temperatures is shown in Table 4.4 and Figure 4.6.

Table 4.4 Effect of the polymerization temperature on the water absorbency (Q) of the synthesized copolymers at 99/1, 97/3, and 95/5 mole ratios of AM/IA*

Temperature (°C)	Water absorbency (Q) (g g^{-1})		
	AM/IA: 99/1	AM/IA: 97/3	AM/IA : 95/5
40	264±18	356±4	589±17
50	372±9	394±9	640±7
60	128±18	311±12	355±20

*Polymerization was carried out at 0.2%mole of N-MBA, 0.3%mole of APS, 1.2% mole of TEMED and 30 min.

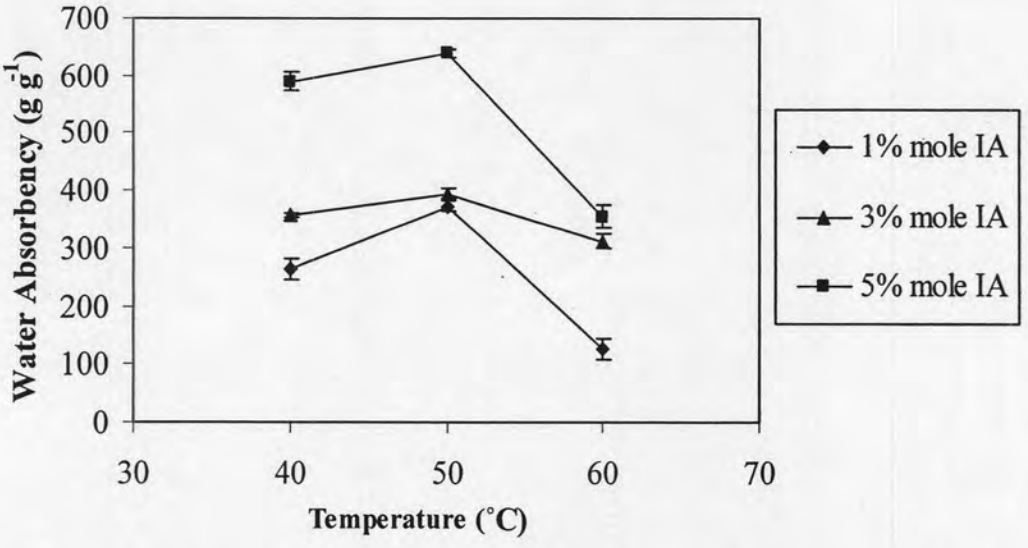

Figure 4.6 Effect of the polymerization temperature on the water absorbency (Q) of the synthesized poly(AM-*co*-IA) copolymers at various IA concentrations with 0.2% mole of N-MBA, 0.3% mole of APS, 1.2% mole of TEMED and 30min.

The water absorbency of the poly(AM-*co*-IA) copolymer is also greatly influenced by the polymerization temperature as shown in Figure 4.6. When the temperature was lower than 50°C, the water absorbency decreased. However, the water absorbency decreased if the polymerization temperature was increased further. Since the dissociation rate of APS initiator with the diamine co-initiator (TEMED) is high at the moderately high temperature (50°C) due to the prominent characteristic of a redox initiator. The rate of copolymerization is thus enhanced (36). In addition, the rate of diffusion of AM and IA to the macro radicals is increased at higher temperatures. This in turn resulted in a higher degree of polymerization and consequently higher water absorbency of the polymer produced. When the polymerization temperature was too high, the radical termination reaction are enhanced that the absorbency is decreased instead. The absorbency of the polymer reached its optimum value when the reaction was carried out at 50°C.

. 4.2 Effects of Influential Parameters on Absorbency of Poly(AM-*co*-IA)/mica Nanocomposites

4.2.1 Effect of Itaconic Acid Concentration on Water Absorbency

The water absorbency of the superabsorbent nanocomposite, synthesized by 99/1, 98/2, 97/3, 96/4 and 95/5 mole ratios of AM/IA with 0.2% mole of N-MBA, 0.3% mole of APS, 1.2% mole of TEMED, at mica content of 2, 5, 10 and 15% wt, is shown in Table 4.5 and Figure 4.7.

Table 4.5 Effect of itaconic acid concentration on water absorbency (Q) of the synthesized nanocomposite*

Mica Content (%wt)	Water absorbency (Q) (g g^{-1})				
	AM/IA:99/1	AM/IA:98/2	AM/IA:97/3	AM/IA:96/4	AM/IA:95/5
0	372±9	383±14	394±9	476±6	640±7
2	340±18	327±6	390±6	501±13	690±16
5	350±5	350±3	442±12	601±20	748±5
10	288±9	319±4	424±2	484±6	635±18
15	260±3	305±14	391±10	529±23	570±16

*Polymerization was carried out at 0.2% mole of N-MBA, 0.3% mole of APS, 1.2% mole of TEMED, 50°C, and 30min.

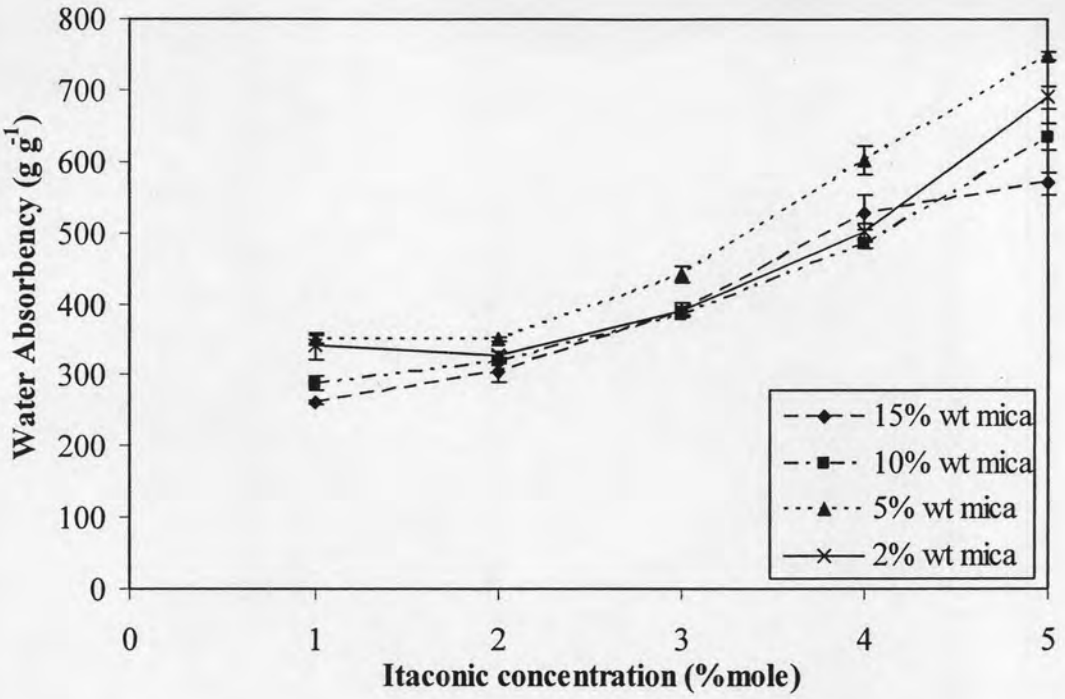

Figure 4.7 Effect of the itaconic acid concentration on the water absorbency (Q) of the synthesized poly(AM-*co*-IA)/mica nanocomposite at 0.2% mole of N-MBA, 0.3% mole of APS, 1.2% mole of TEMED, 50°C and 30 min with mica contents at 2, 5, 10, 15% wt.

Effect of IA concentration on water absorbency of the synthesized superabsorbent nanocomposites is shown in Table 4.5 and Figure 4.7. The water absorbency of superabsorbent nanocomposites shows a similar trend as that of poly(AM-*co*-IA) copolymer in which the water absorbency increases with an increase in IA concentration. The reason is that the addition of IA simultaneously enhances a hydrophilic incorporation from carboxylic groups (-COOH) into the polymer network, resulting in an electrostatic repulsive force between the charge sites on carboxylate ions upon their complete dissociation, thus the network is expanded. At 5% mole of IA concentration, the highest swelling of the superabsorbent polymer nanocomposites was also achieved.

4.2.2 Effect of Mica Content

4.2.2.1 Effect of Mica Content on Water Absorbency

The water absorbency of the superabsorbent nanocomposites, synthesized by 99/1, 98/2, 97/3, 96/4, and 95/5 mole ratios of AM/IA with 0.2% mole of N-MBA, 0.3% mole of APS, 1.2% mole of TEMED, and various mica contents, is shown in Table 4.5 and Figure 4.8.

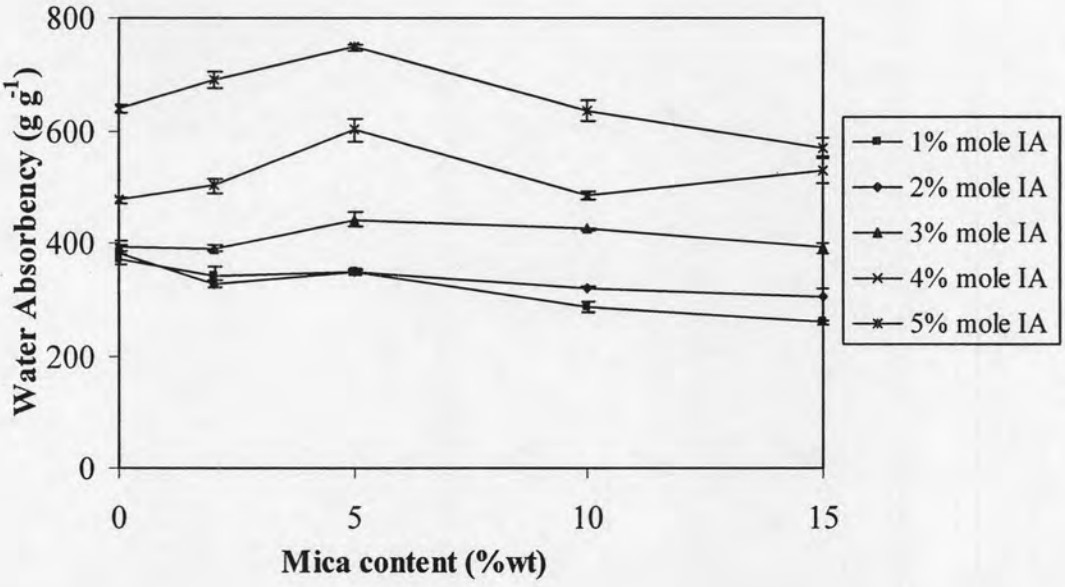

Figure 4.8 Effect of mica content on water absorbency (Q) of the synthesized poly(AM-*co*-IA)/mica nanocomposites at various mica contents, 0.2% mole of N-MBA, 0.3% mole of APS, 1.2% mole of TEMED, 50°C, and 30 min.

The results are shown in Table 4.5 and Figure 4.8 in which the water absorbency increases with mica content, which content is not greater than 5% wt. The effect is more pronounced when IA is larger than 3% mole and at maximum at 5% mole. According to Flory's swelling theory, the water absorbency for the polymer is dependent on the affinity of the gel toward water (37). It was observed that the

strongest affinity was found at 5%wt mica. Below 5% wt mica, the effect of affinity on mica was not so strong; thus the water absorbency depended on the amount of IA in the copolymer. For this reason, adding a small amount of mica into the copolymer can increase the affinity of the polymer to absorb more water; therefore the absorbency of the copolymer increased. However, above 5% wt of mica content (see the next section), a small decline in the water absorbency was seen, suggesting a small effect from the added mica on the copolymer absorbency. This is due to the reason that the intercalated structure occurred in the composite and the grafting mechanism could take place on the surface of mica, as described in the following sections. It suggests that a greater amount of mica created more crosslink points, which increased the crosslink density of superabsorbent nanocomposites and less space was left for water to enter.

4.2.2.2 Effect of Mica Content on Absorbency Under Load

The water absorbency under load (0.28 psi. and 0.70 psi.) of the poly(AM-*co*-IA)/mica nanocomposites, synthesized by 99/1, 97/3, and 95/5 mole ratios of AM/IA with 0.2% mole of N-MBA, 0.3% mole of APS, 1.2% mole of TEMED at various mica contents (%wt) is shown in Table 4.6 and Figure 4.9.

Table 4.6 Effect of mica content on absorbency under load (AUL) of the synthesized poly(AM-*co*-IA)/mica nanocomposites*

Mica content (%wt)	absorbency under load (AUL) ($g\ g^{-1}$)	
	0.28 psi.	0.7 psi.
0	8.88±0.49	8.21±0.6
2	10.71±1.28	9.34±0.91
5	10.68±1.09	8.31±1.23
10	12.67±0.12	10.88±0.38
15	13.33±1.15	10.17±0.81

*Polymerization was carried out at various mica contents, AM/IA ratio 99/1, 0.2% mole of N-MBA, 0.3% mole of APS, 1.2% mole of TEMED, 50°C and 30 min.

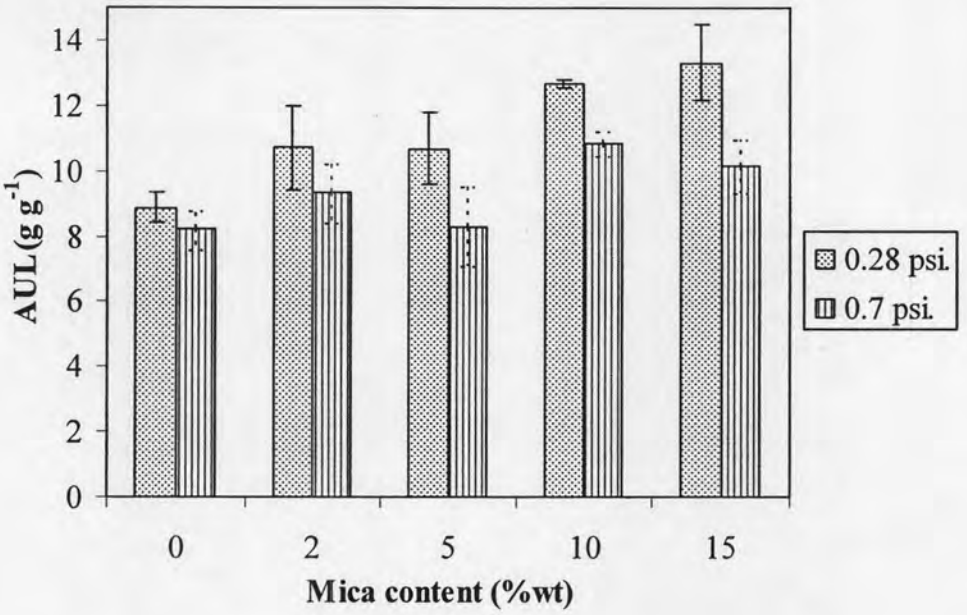

Figure 4.9 Effect of mica content on absorbency under load (AUL) of the synthesized poly(AM-*co*-IA)/mica nanocomposites at various mica contents, AM/IA 99/1, 0.2% mole of N-MBA, 0.3% mole of APS, 1.2% mole of TEMED, 50°C, and 30 min.

Absorbency under load (AUL) measures the ability of a polymer to absorb fluid under a static load, and can be considered as a measurement of gel stability or gel strength. A high value of AUL correlates to a high gel strength. The water absorbency under load (0.28 and 0.7 psi) of the poly(AM-*co*-IA)/mica nanocomposites is drastically reduced compared to the one without a load as shown in Figure 4.8. Interestingly, the water absorbency under load (AUL 0.28 and 0.7 psi) increased with the mica content as shown in Figure 4.9. It may be attributed to the fact that mica particles act as crosslink points. When the contents of mica increased, the crosslink density was increased, gel strength was sufficiently improved at the expense of high water absorption.

4.2.3 Effect of Mica Content on Viscoelastic Properties of Poly(AM-*co*-IA)/mica Nanocomposite

The plot of G'(γ) and G''(γ) of poly(AM-*co*-IA)/mica composite at various mica contents is given in Figure 4.10.

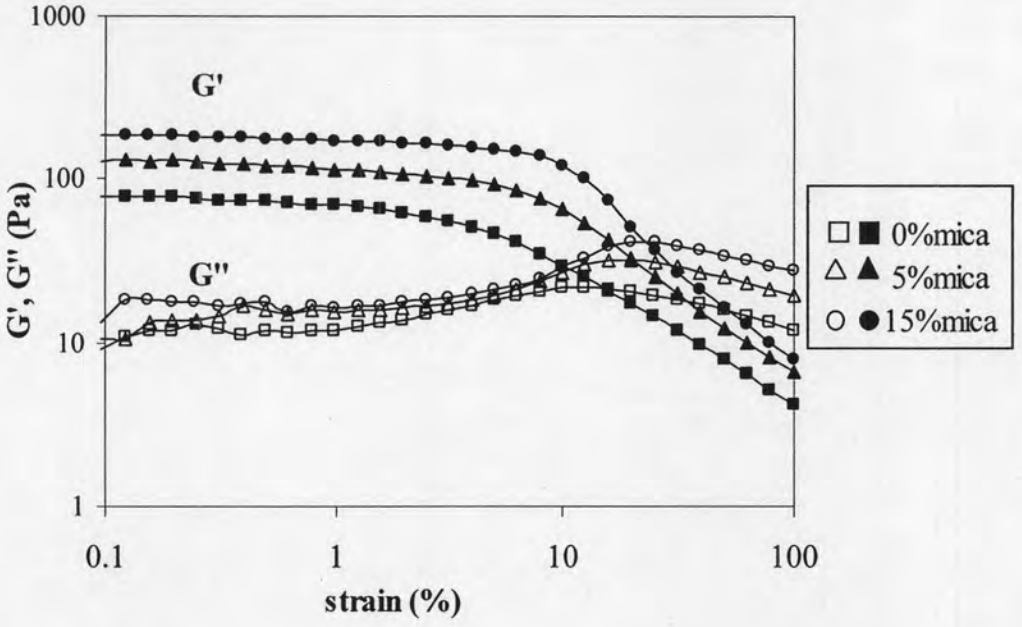

Figure 4.10 Strain dependence of G' and G'' at the constant angular frequency (1 rad/s) for the synthesized poly(AM-*co*-IA)/mica nanocomposites at various mica contents, at AM/IA ratio of 99/1, 0.2% mole of N-MBA, 0.3% mole of APS, 1.2% mole of TEMED, 50°C, and 30 min.

The effect of shear strain on the measured G' and G'' at the constant frequency (ω = 1 rad/s) is shown in Figure 4.10. Below 1% deformation, it was observed that G'(ω) is independent of the applied strain, similar to that of the copolymer gel. As a result, the frequency sweep test was carried out between 0.1 and 100 rad/s. The plot of G'(ω) and G''(ω) is given in Figure 4.11.

The effect of frequency on the measured G' and G'' at the strain ($\gamma = 1\%$) was performed and shown in Figure 4.11. The impressive strength (or "gel strength") of these swollen polymer composites could be indicated by the magnitudes of $G'(\omega)$, as explained earlier. The fact that $G' >> 0$ reflects a substantial presence of true solids (clay and rubber-like chain), and also the existence of a network structure, composed of the crosslinked polymer and the clay linkage sites (34). This indicates that the increase in mica content increases the G', which is corresponding to the increase in gel strength. The magnitudes of G' are increased from 0% to 15% wt of mica. The value are in the amounts of 63, 104, and 159 Pa (at 0.1% strain) for 0, 5 and 15% mica added, respectively. The G' increments were observed at 64 and 153% based on 0% mica Therefore, only 5%wt mica addition can enhance the G' value more than 50%. Moreover, this result also conformed to the effect of mica content on absorbency under load.

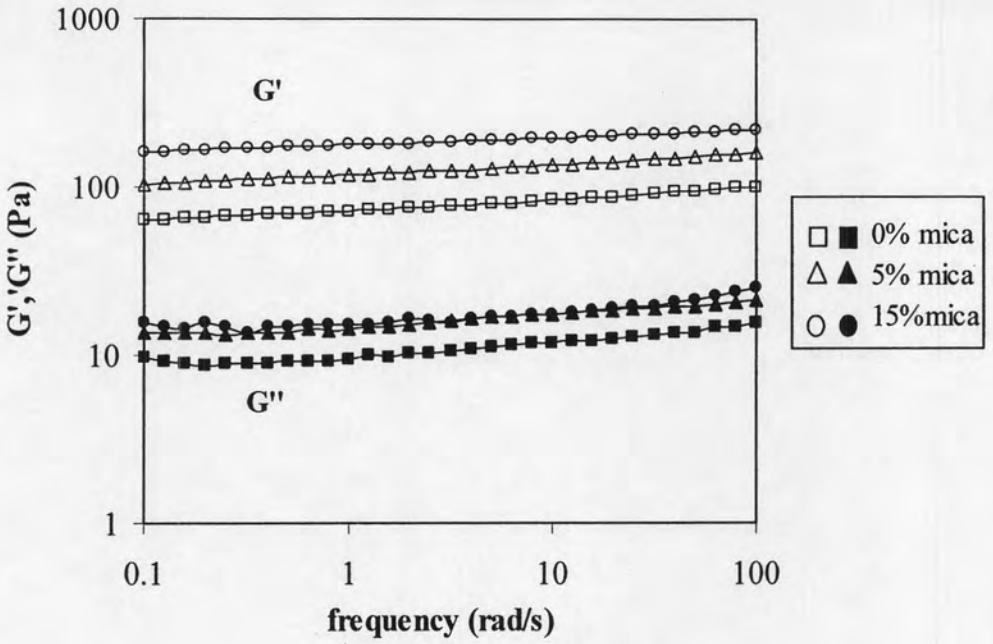

Figure 4.11 Angular frequency dependence of G' and G'' at the constant strain (1% strain) for the synthesized poly(AM-*co*-IA)/mica nanocomposites at the AM/IA ratio of 99/1, 0.2% mole of N-MBA, 0.3% mole of APS, 1.2% mole of TEMED, at various mica contents, 50°C, and 30 min.

4.2.4 Effect of *N,N'*-methylenebisacrylamide Concentration

The water absorbency of the superabsorbent nanocomposite, synthesized by 99/1, 97/3 and 95/5 mole ratios of AM/IA with 0.3% mole of APS, 1.2% mole of TEMED, at mica contents of 5 and 15% wt, and various concentrations of the N-MBA crosslinker is shown in Table 4.7, Figures 4.12 to 4.14.

Table 4.7 Effect of crosslinker concentration on water absorbency (Q) of the synthesized nanocomposites*

Concentration of N-MBA (%mole)	Water absorbency (Q) (g g^{-1}) at mica contents (%wt) for					
	AM/IA 99/1		AM/IA 97/3		AM/IA 95/5	
	5%	15%	5%	15%	5%	15%
0.2	350±4	260±3	442±12	391±10	785±5	570±16
0.5	124±7	172±8	247±10	245±4	359±10	447±6
0.7	95±3	96±4	156±4	199±2	232±2	207±2
0.9	80±4	80±3	127±1	131±3	172±4	149±5

*Polymerizations were carried out at AM/IA ratio of 99/1, 97/3 and 95/5, 0.3% mole of APS, 1.2% mole of TEMED, mica contents at 5 and 15% wt, and various concentrations of the N-MBA crosslinker, 50°C, and 30 min.

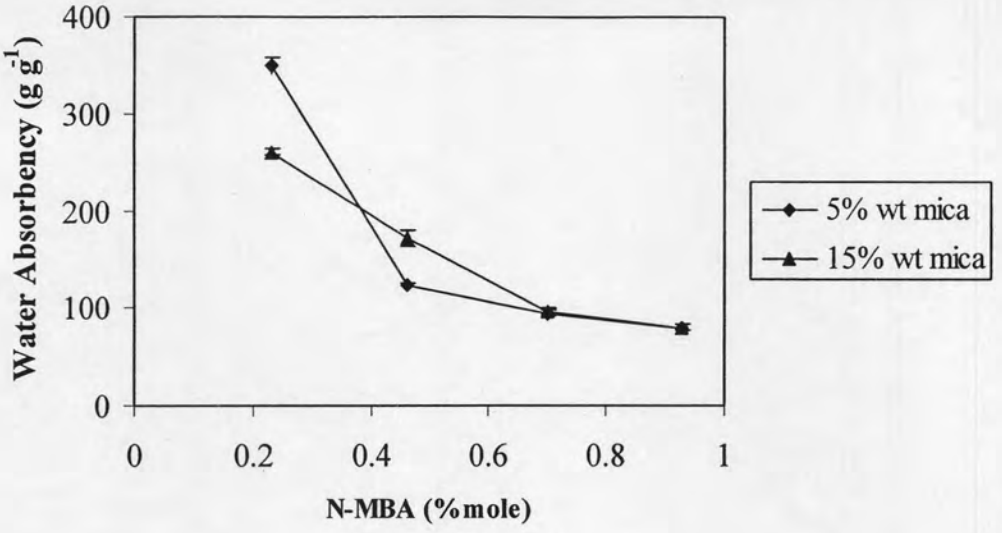

Figure 4.12 Effect of crosslinker concentration on water absorbency (*Q*) of the synthesized poly(AM-*co*-IA)/mica nanocomposite at AM/IA mole ratio 99/1, 0.3% mole of APS, 1.2% mole of TEMED, 50°C, and 30 min, mica contents at 5 and 15% wt.

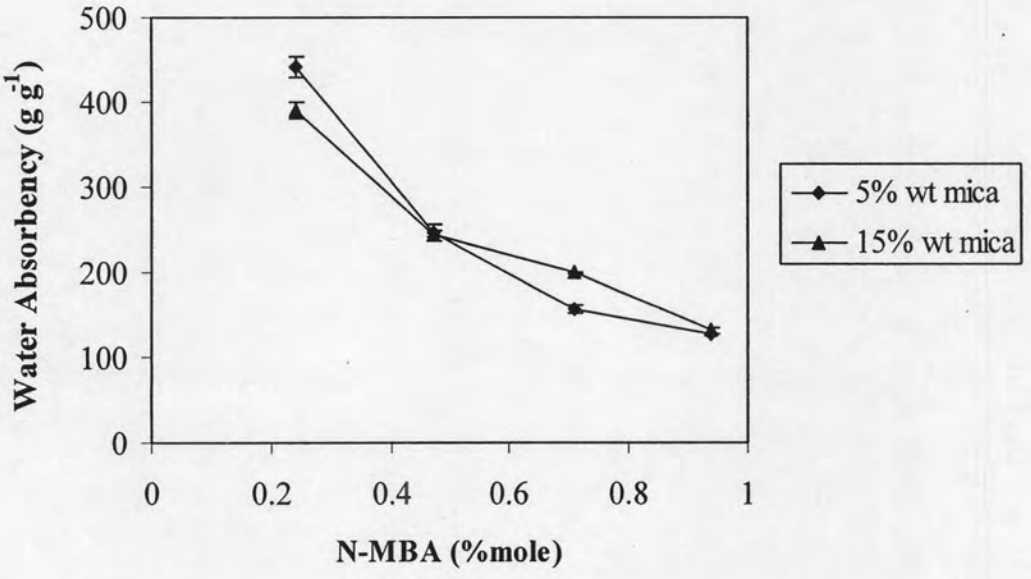

Figure 4.13 Effect of the crosslinker concentration on water absorbency (*Q*) of the synthesized poly(AM-*co*-IA)/mica nanocomposite at AM/IA mole ratio 97/3, 0.3% mole of APS, 1.2% mole of TEMED, 50°C, and 30 min, mica contents at 5 and 15% wt.

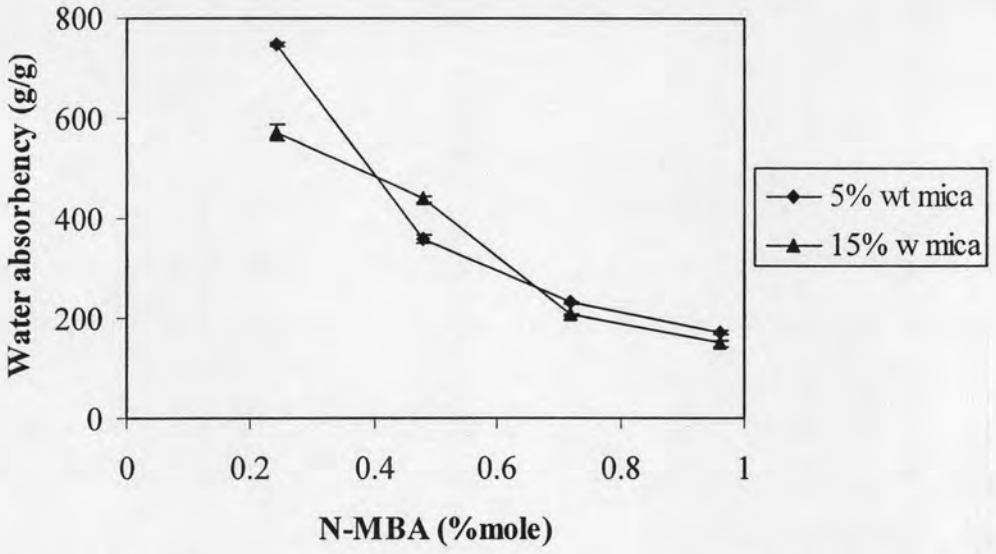

Figure 4.14 Effect of the crosslinker concentration on water absorbency (Q) of the synthesized poly(AM-*co*-IA)/mica nanocomposite at AM/IA mole ratio 95/5, 0.3% mole of APS, 1.2% mole of TEMED, 50°C, and 30 min, mica contents at 5 and 15% wt.

The effect of crosslinker concentration on water absorbency of nanocomposites is illustrated in Table 4.7 and Figures 4.12 to 4.14. The relationship between the absorbency and network structure parameters was investigated by Flory and given in the Equation (2.1). This relationship may be applied to the present nanocomposite, because the crosslinked poly(AM-*co*-IA) may be considered as a part of the network. Therefore, Equation (2.1) can also be applied to explain these results. When the crosslinker concentrations increased, the chemical crosslinking density of the superabsorbent nanocomposites also increased. This would result in a greater decrease in the spaces between the copolymer chains and lead to a decrease in water absorbency of composite.

4.2.5 Effect of the Polymerization Temperature

The water absorbency of the superabsorbent nanocomposites, synthesized by 99/1, 97/3 and 95/5 mole ratios of AM/IA with 0.2% mole of N-MBA, 0.3% mole of APS, 1.2% mole of TEMED, mica contents at 5 and 15% wt, and various polymerization temperatures is shown in Table 4.8 and Figures 4.15 to 4.17.

Table 4.8 Effect of the polymerization temperature on the water absorbency (Q) of the synthesized nanocomposites at 99/1, 97/3, and 95/5 mole ratios of AM/IA*

Temperature (°C)	Water absorbency (Q) (g g^{-1}), at mica content (%wt) for					
	AM/IA 99/1		AM/IA 97/3		AM/IA 95/5	
	5%	15%	5%	15%	5%	15%
40	239±12	204±7	391±5	289±10	691±19	502±7
50	350±5	260±3	442±12	391±10	748±5	570±16
60	204±16	121±8	374±2	281±13	416±14	359±9

*Polymerizations were carried out at AM/IA ratio of 99/1, 97/3 and 95/5, 0.2% mole of N-MBA, 0.3% mole of APS, 1.2% mole of TEMED, mica contents at 5 and 15% wt, 50°C, and 30 min.

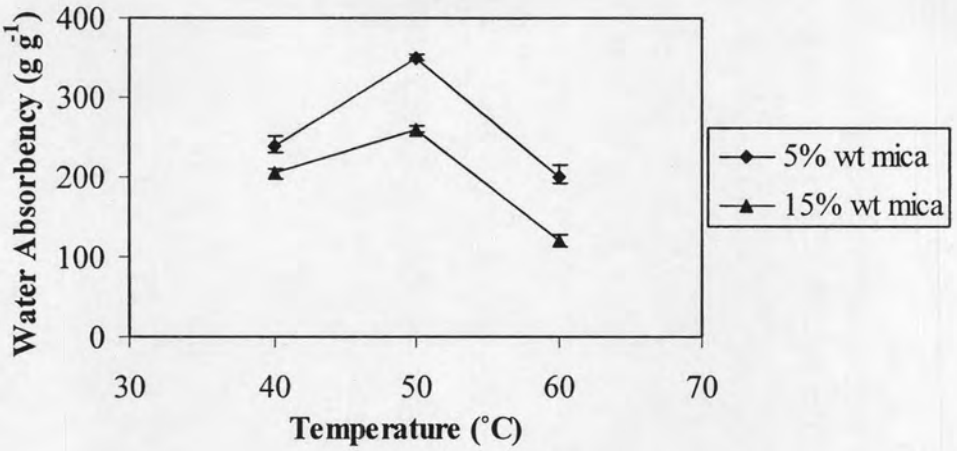

Figure 4.15 Effect of the polymerization temperature on the water absorbency (Q) of the synthesized poly(AM-*co*-IA)/mica nanocomposites at AM/IA mole ratio 99/1, 0.3% mole of APS, 1.2% mole of TEMED, 50°C, and 30 min, mica contents at 5 and 15% wt.

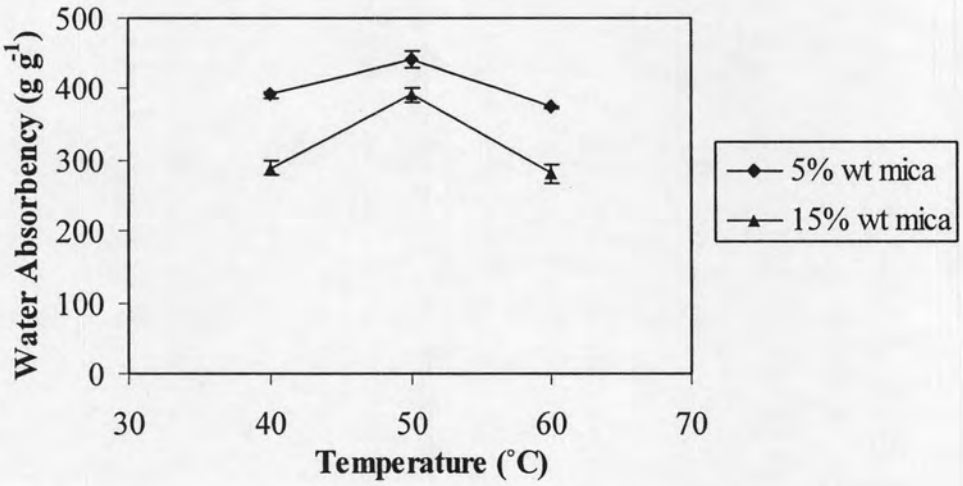

Figure 4.16 Effect of the polymerization temperature on the water absorbency (Q) of the synthesized poly(AM-*co*-IA)/mica nanocomposites at AM/IA mole ratio 97/3, 0.3% mole of APS, 1.2% mole of TEMED, 50°C, and 30 min, mica contents at 5 and 15% wt.

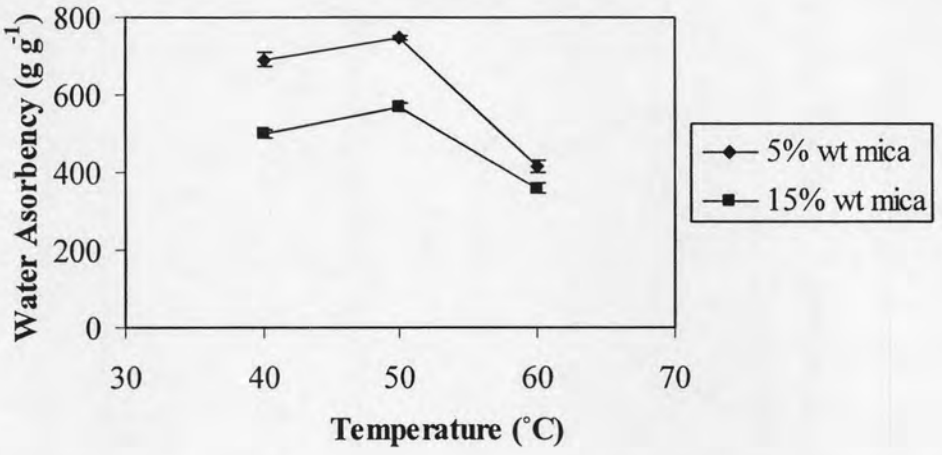

Figure 4.17 Effect of polymerization temperature on the water absorbency (Q) of the synthesized poly(AM-*co*-IA)/mica nanocomposites at AM/IA mole ratio 95/5, 0.3% mole of APS, 1.2% mole of TEMED, 50°C, and 30 min, mica contents at 5 and 15% wt.

The water absorbency of the poly(AM-*co*-IA)/mica nanocomposites is also greatly influenced by the polymerization temperature as shown in Table 4.8 and Figures 4.15 to 4.17. The absorbency of the polymer reached its maximum value when the reaction was carried at 50°C. This phenomenon had been explained previously in the Section of poly(AM-*co*-IA) copolymer.

4.3 Water Absorbency of the Superabsorbent Nanocomposites in Artificial Urine

The water absorbency of the superabsorbent nanocomposites prepared with AM/IA ratio of 99/1, 97/3, and 95/5, at various mica contents were measured in artificial urine and shown in Table 4.9 and Figure 4.18

Table 4.9 The water absorbency in artificial urine of the synthesized superabsorbent polymer nanocomposites*

Mica content (% wt)	Water absorbency (Q) (g g^{-1})		
	AM/IA 99/1	AM/IA 97/3	AM/IA 95/5
0	51±3	69±3	72±2
2	51±5	69±2	79±3
5	46±1	64±2	76±2
10	48±3	63±2	63±3
15	45±4	58±2	51±1

*Polymerizations were carried out at AM/IA ratio of 99/1, 97/3 and 95/5, 0.2% mole of N-MBA, 0.3% mole of APS, 1.2% mole of TEMED, at various mica contents, 50°C, and 30 min.

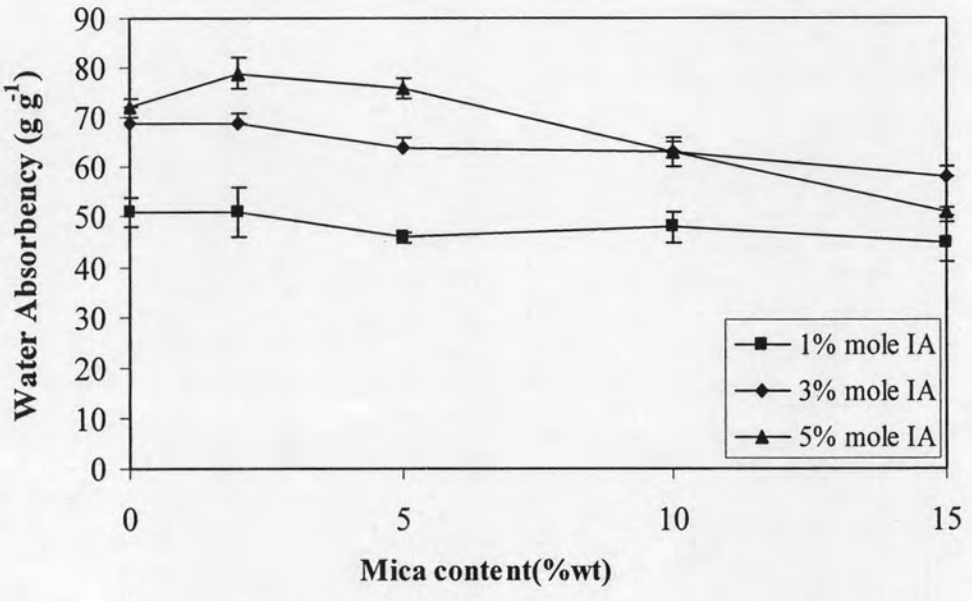

Figure 4.18 Water absorbency in artificial urine of the superabsorbent nanocomposites at AM/IA ratio of 99/1, 97/3 and 95/5, 0.2% mole of N-MBA, 0.3% mole of APS, 1.2% mole of TEMED, at various mica contents, 50°C, and 30 min.

The most important property in a commercial superabsorbent used in personal care applications is the extent swelling (38). An acceptable swelling capacity is approximately 20-40 g of urine per gram of polymer. The amount of urine absorbed by various poly(AM-*co*-IA)/mica nanocomposites was investigated and the results are illustrated in Table 4.9 and Figure 4.18. In general, the swelling of the superabsorbent nanocomposite in artificial reference urine is much lower than the swelling obtained in distilled water as shown in Figure 4.8. This nature is due to a decrement in the expansion of the gel networks, which is caused by the repulsive forces of counter ions on the polymeric chain shielded by the bound ionic charges. Therefore, the osmotic pressure difference between the gel network and the external solution decreased with an increase in the ionic strength of artificial urine (39). The forces for the absorption of ionic solutions are attributed to the osmotic pressure based on the movable counter ions, the polymer-solvent affinity and the rubber elasticity. The effect of ionic strength on the water absorbency can be expressed by Flory's equation as shown in Equation (2.1) in which the artificial urine has ionic strength of about 0.0747 mol-ion dm^{-3}. The ionic strength of the swollen liquid has an inversely proportional effect on equilibrium swelling ratio. The tendency of artificial urine absorption thus slightly decreases with increasing the content of mica in the poly(AM-*co*-IA)/mica nanocomposites. At the AM/IA of 95/5 with 2% of mica content, the water absorbency in artificial urine of this superabsorbent nanocomposite is at maximum ($\approx$ 80 g g^{-1}) which meets the commercial requirement of this type of product.

4.4 Characterization

4.4.1 FT-IR Spectra of Mica, the Synthesized Copolymer and Nanocomposites

The FTIR spectra of mica, poly[acrylamide-*co*-(itaconic acid)] and poly[acrylamide-*co*-(itaconic acid)]/mica nanocomposites are shown in Figures 4.19 to 4.23, and in Table 4.10. The strong peak of the COO^- group observed at 1665-1664 cm^{-1} in Figures 4.21 to 4.23 and the absorption band at 1016-1011 cm^{-1} and 473-471 cm^{-1} designates the existence of Si-OH group. These peaks confirm that the reaction product is the desired composites (20). The absorption peaks at 1659 cm^{-1} (Figure 4.20 and 4.23 (d)) attributed to the $-COO^-$ group on the IA has experienced a conformation change during the reaction (19). The absorption peaks at 1003 and 476 cm^{-1} contributed to Si-OH group on mica (Figures 4.19 and 4.23 (a)) also have acquired a conformation change during the reaction. Since the characteristic absorption peak for $-COO^-$ group on the IA and Si-OH group has changed after the copolymerization, it is suggested that the reaction between Si-OH group on mica and $-COO^-$ group on the IA takes place during the copolymerization (19). The possible reaction is the grafting reaction (esterification reaction) of OH groups on mica with $-COO^-$ group on the IA (6, 20). The grafting is presumed that the OH groups in mica may react with IA, and then radical chain polymerization takes place (Figure 4.24, Mechanism I). Another possible mechanism is that the hydroxyl groups may react with radicals and liberate free radicals on the mica structure; thus the graft polymerization will take place on these free radicals, giving IA-AM branches on the mica backbone as given in the mechanism II (Figure 4.24) (20).

The absorption bands at 1659 cm^{-1} in Figure 4.20, 1664 cm^{-1} in Figure 4.21, and 1665 cm^{-1} in Figure 4.22 attributed to the $-COO^-$ group. The absorption band of

$-COO^-$ shifted to a slightly higher wave number when the content of mica is higher. Moreover, with increasing mica content, the absorption band of -C-N stretching ($-CONH_2$) was shifted from 1448 cm^{-1} to 1450 cm^{-1}. Such information indicates that the content of mica has an influence on the interaction between AM/IA and mica, and then on swelling properties of the corresponding superabsorbent nanocomposites. In addition, grafting mechanisms as proposed in Figure 4.24 could be possible for the polymer chains to graft on the mica surface.

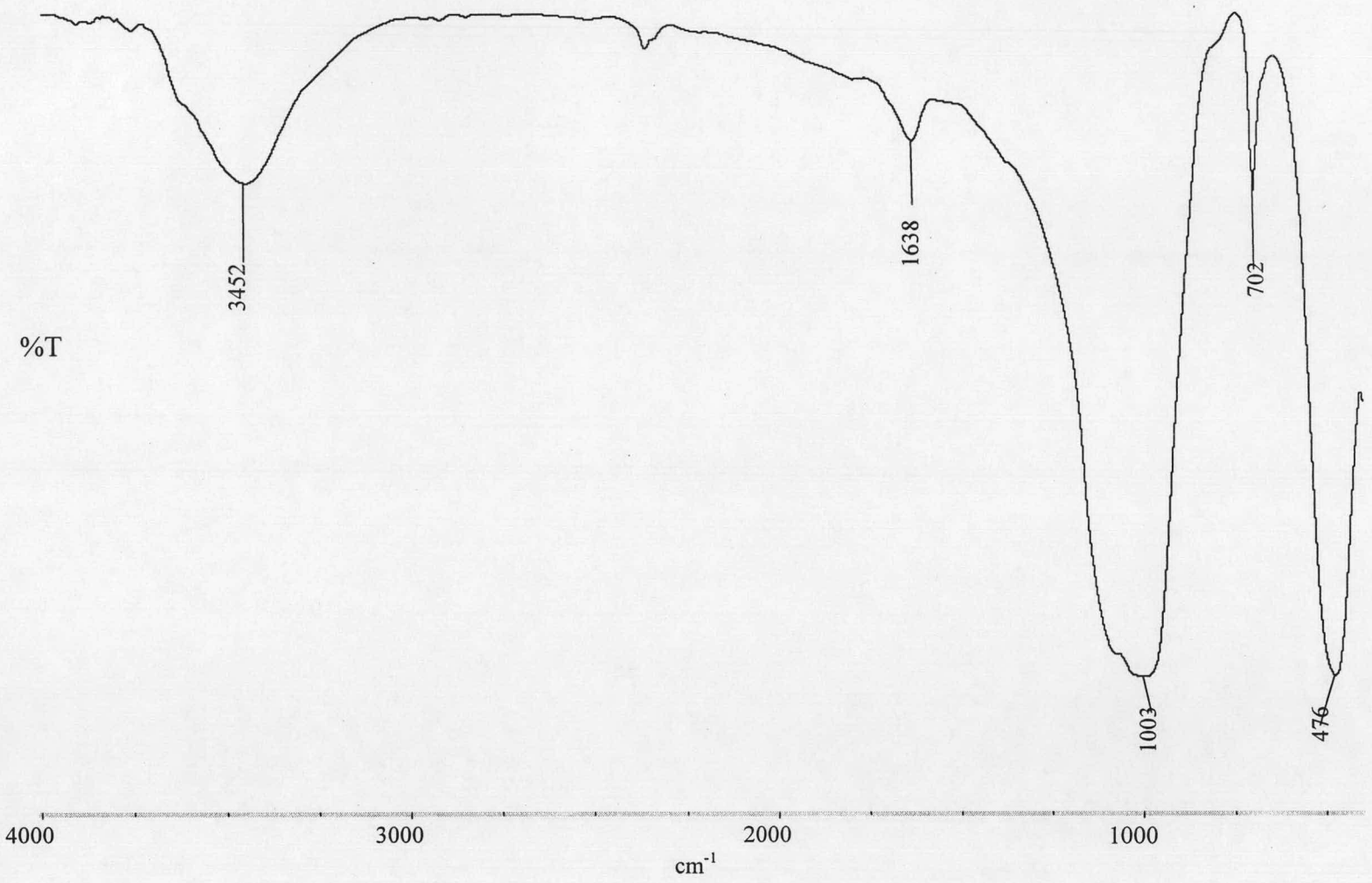

Figure 4.19 FT-IR spectrum of mica.

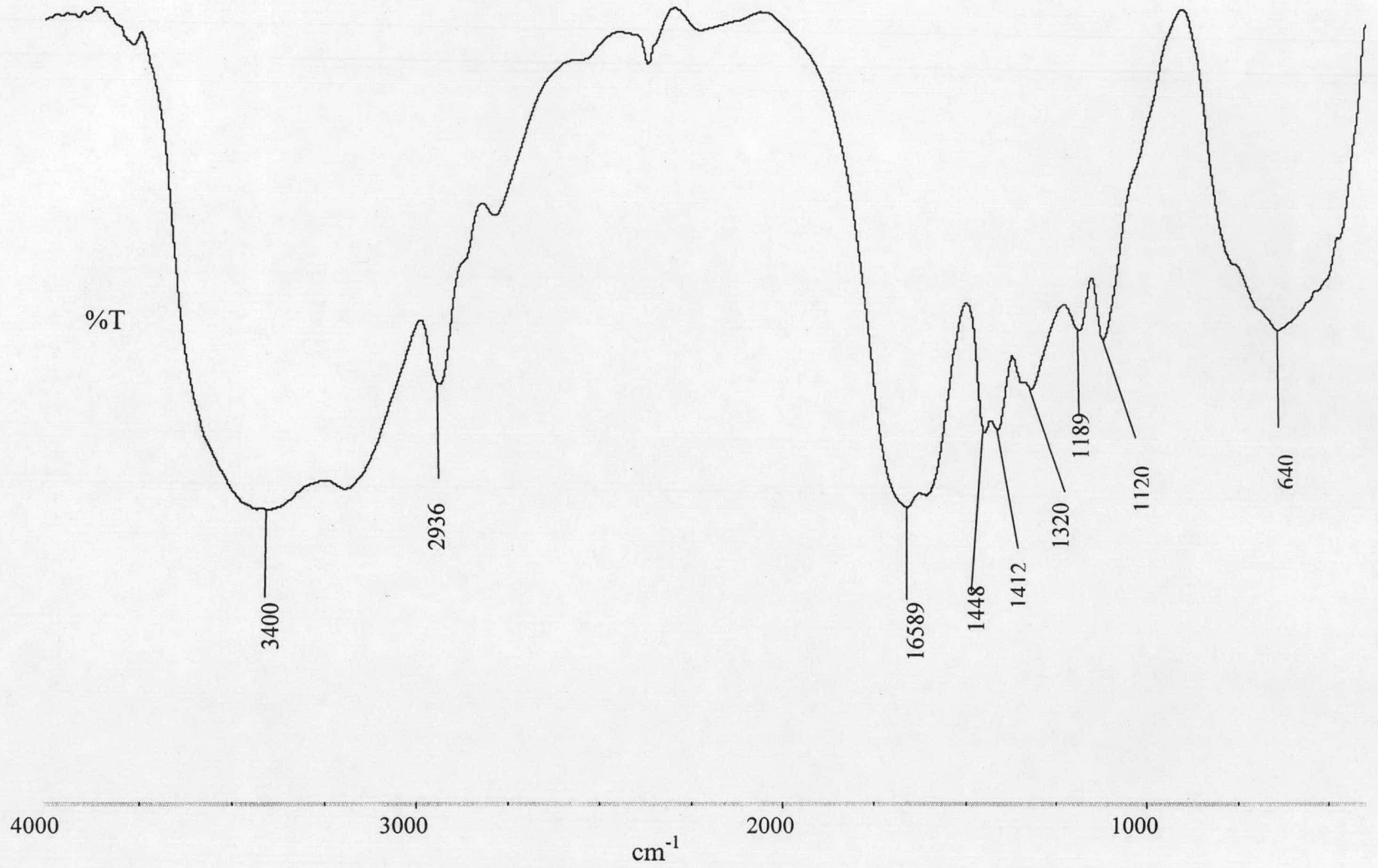

Figure 4.20 FT-IR spectrum of the synthesized poly(AM-*co*-IA) copolymer.

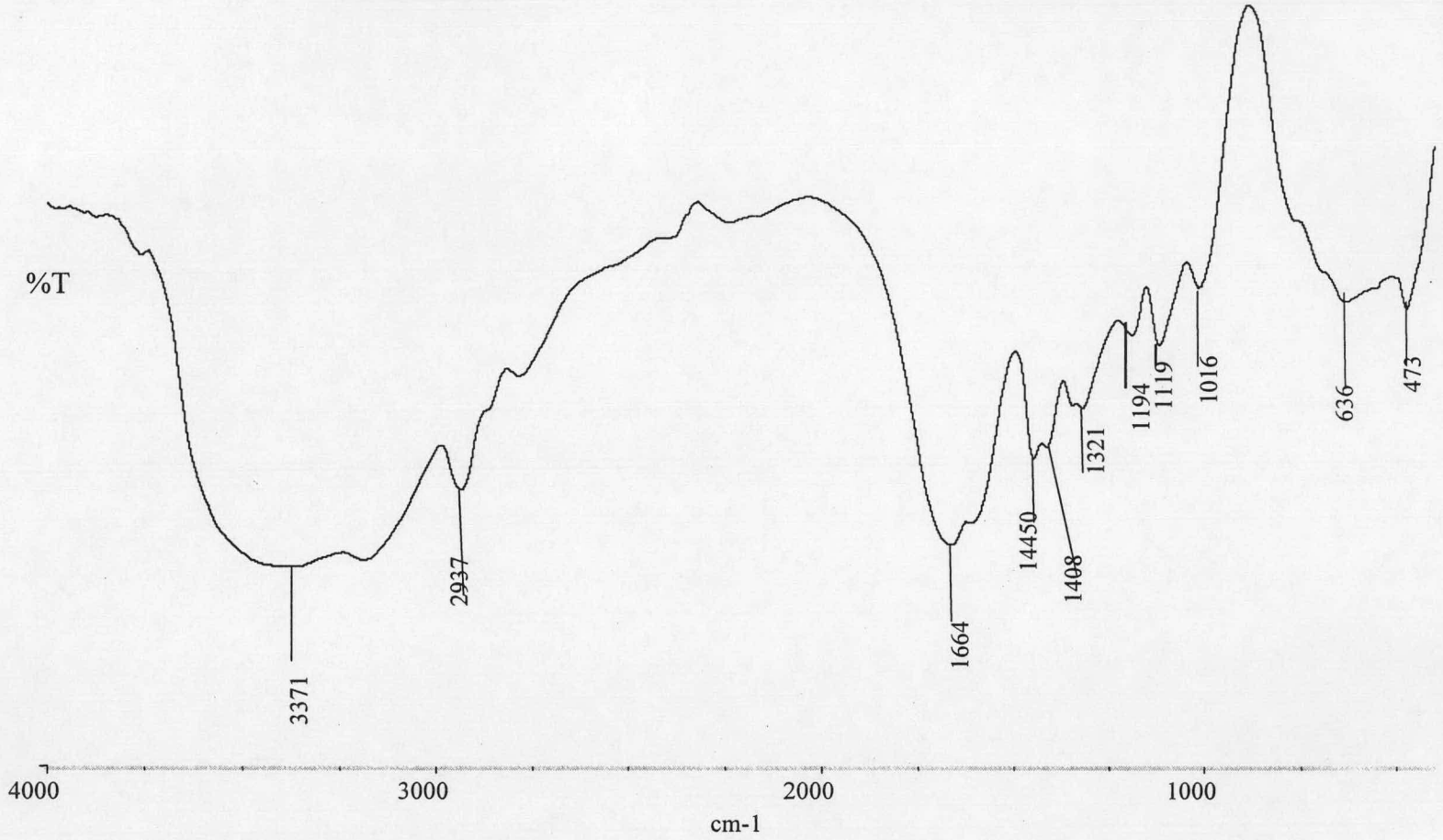

Figure 4.21 FT-IR spectrum of the synthesized poly(AM-*co*-IA)/mica nanocomposites with 5% wt of mica.

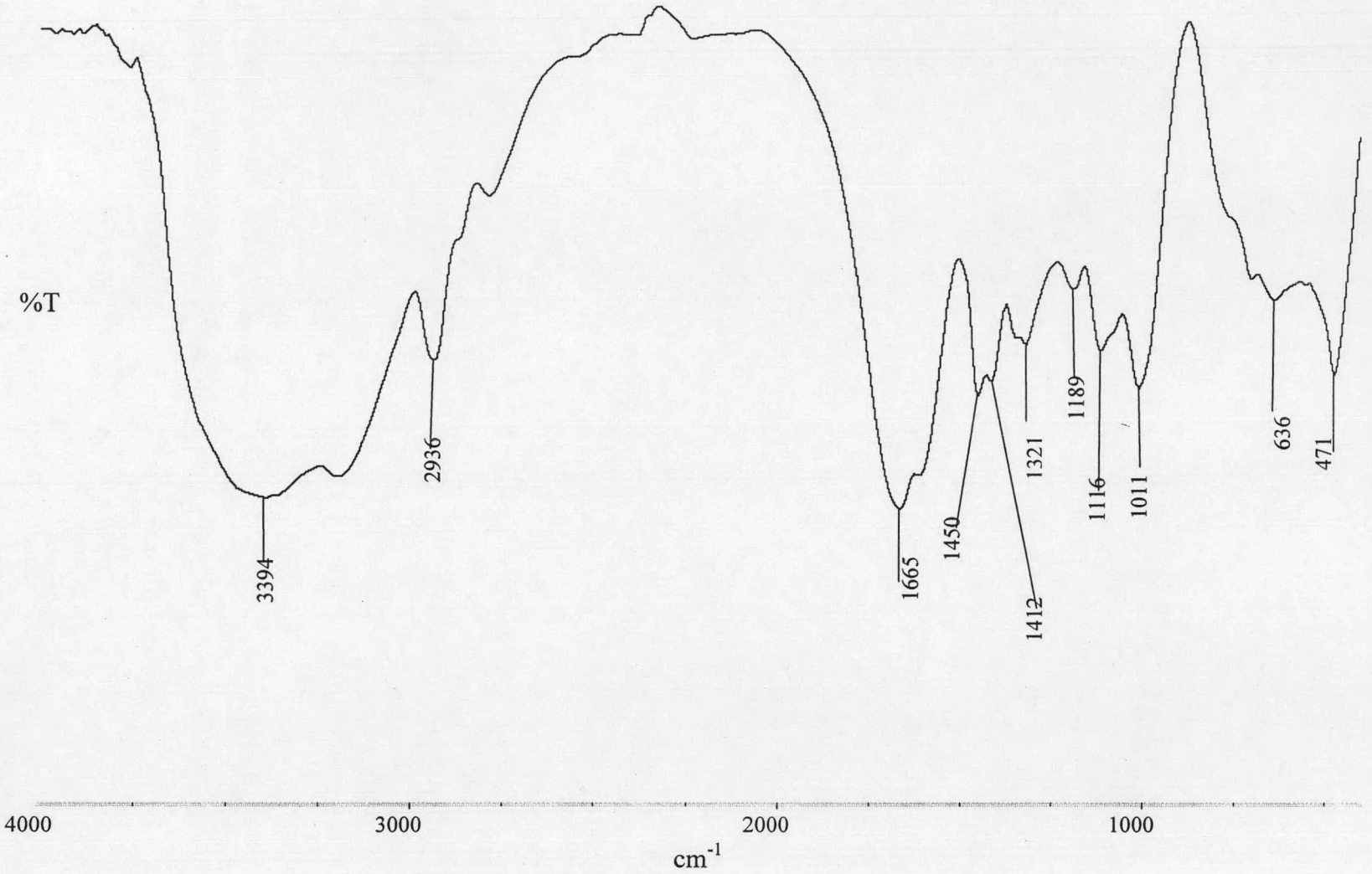

Figure 4.22 FT-IR spectrum of the synthesized poly(AM-*co*-IA)/mica nanocomposites with 15% wt of mica.

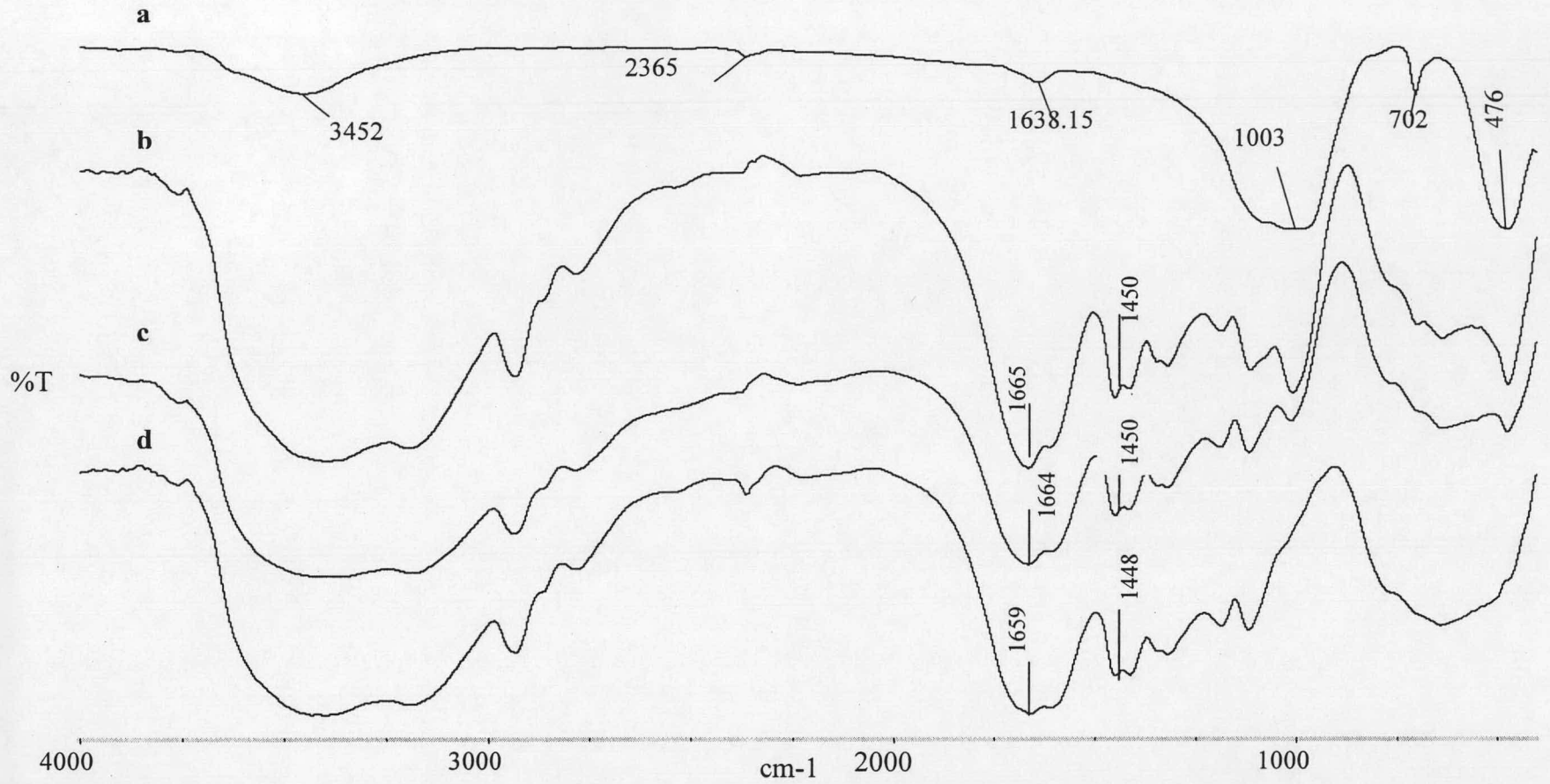

Figure 4.23 FT-IR spectra of (a) mica, (b), (c) poly(AM-*co*-IA)/mica nanocomposites with 15 and 5% wt of mica, respectively, and (d) poly(AM-*co*-IA) copolymer.

Table 4.10 Assignments for the FTIR spectra of mica (5), synthesized poly(AM-*co*-IA), poly(AM-*co*-IA)/mica nanocomposite with 5% wt mica and poly(AM-*co*-IA)/mica nanocomposite with 15% wt mica

Mica		Poly(AM-*co*-IA)		Poly(AM-*co*-IA)/mica nanocomposite with 5% wt mica		Poly(AM-*co*-IA)/mica nanocomposite with 15% wt mica	
Wave number (cm^{-1})	Assignment	Wave number (cm^{-1})	Assignment	Wave number (cm^{-1})	Assignment	Wave number (cm^{-1})	Assignment
3451, strong	O-H stretching	3401, strong	O-H stretching	3372, strong	O-H stretching	3393, strong	O-H stretching
1638, weak	interlayer water of mica vibration						
		2936, sharp and strong	C-H stretching CH_3 and CH_2 (aliphatic)	2937, sharp and strong	C-H stretching CH_3 and CH_2 (aliphatic)	2936, sharp and strong	C-H stretching CH_3 and CH_2 (aliphatic)
1003, strong	Si-O stretching			1016, weak	Si-O stretching	1011, weak	Si-O stretching
		1659, strong	C=O stretching of COO-	1664, strong	C=O stretching of COO-	1665, strong	C=O stretching of COO-
		1448, weak	C-N stretching O=C-NH	1450, weak	C-N stretching O=C-NH	1450, weak	C-N stretching O=C-NH
		1320, weak	C-N aliphatic stretching	1321, weak	C-N aliphatic stretching	1321, weak	C-N aliphatic stretching
702, strong and sharp	Al-O stretching						
476, strong	Si-O bending			473, weak	Si-O bending	471, strong	Si-O bending

Mechanism I

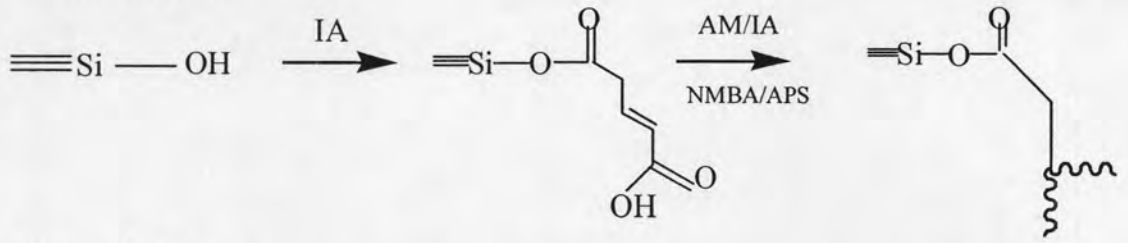

Mechanism II

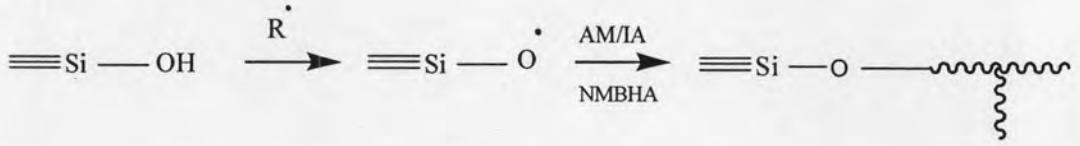

Figure 4.24 Possible grafting mechanism of mica in poly[acrylamide-*co*-(itaconic acid)]/mica nanocomposites.

4.4.2 Nanostructure of Poly(AM-*co*-IA)/mica Composite

4.4.2.1 X-ray Diffraction Analysis

XRD patterns supply very useful information of the gallery size of the final intercalated nanocomposites by measuring the increase of basal (001) d-spacing. Figure 4.25 shows the XRD patterns of mica powder, poly(AM-*co*-IA)/mica nanocomposites with various amounts of mica and poly(AM-*co*-IA) copolymer. The measured d_{001} of mica is 12.44 Å ($2\theta = 7.10°$). The mica composites (AM/IA mole ratio of 97/3 having the composites with 5 and 15 wt% mica) have the peaks observed at about d = 13.78 and 13.96 Å corresponding to $2\theta = 6.41°$ and 6.32, respectively. Further increases in the basal interlayer spacing imply that there is a polymer intercalation within the stacked silicate galleries of mica (4). From the results, a substantial increase in the intensity of the XRD peak is observed for the mica loading from 5 to 15 wt%. This confirmed that the monomer intercalates into the layers of mica.

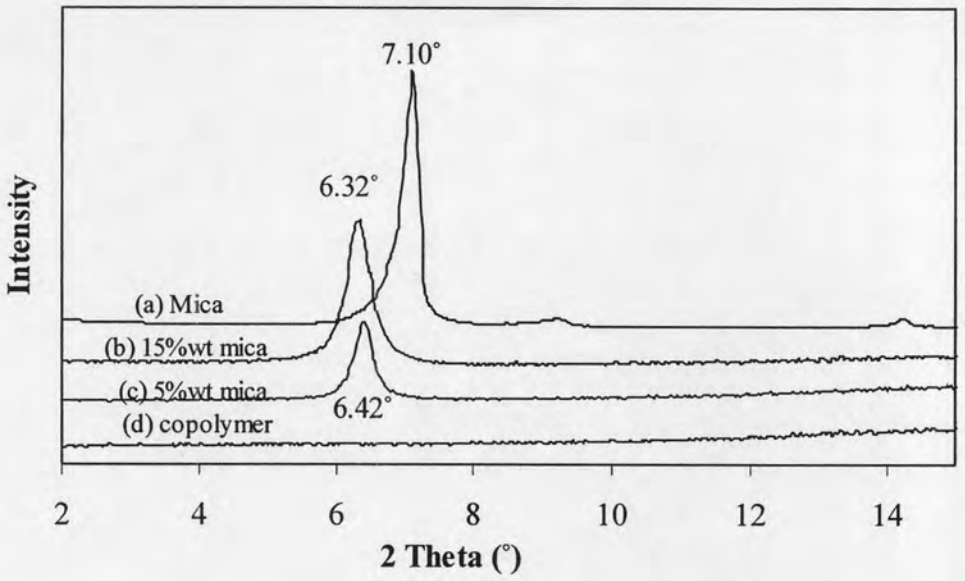

Figure 4.25 X-ray diffraction patterns of (a) Mica powder, (b),(c) poly(AM-*co*-IA)/mica nanocomposites with amounts of mica at 15 and 5wt%, respectively, and (d) poly(AM-*co*-IA) copolymer (AM/IA mole ratio of 97/3).

Table 4.11 summarizes the XRD analysis results showing the changes of 2θ peak positions or (001) basal plane spacing. The tendency of (001) basal plane spacing remained approximately the same at different concentrations. This behavior may be due to the formation of strong hydrogen bonds between the polar groups (carboxyl group) of the repeating units in the polymer, which were intercalated into the interlayer space of silicate layers of mica. Upon the intercalation, the complex was subsequently polymerized in the confined environment of the interlayer space with a free radical initiator (12).

Table 4.11 Summary of X-ray diffraction patterns of the synthesized poly(AM-*co*-IA)/mica nanocomposites at 99/1, 97/3 and 95/5 mole ratios of AM/IA*

AM/IA ratio of composite	Mica content (%)	(001) basal plane spacing (Å)
-	100	12.44
99/1	5	13.94
	15	13.90
97/3	5	13.78
	15	13.96
95/5	5	13.98
	15	13.89

*Polymerizations were carried out at AM/IA ratio of 99/1, 97/3 and 95/5, 0.2% mole of N-MBA, 0.3% mole of APS, 0.2 ml of TEMED, mica contents at 5 and 15% wt, 50°C, and 30 min.

The kinetic and mechanism of the intercalation are complex and are not known in much detail. Gao (7) conjectured that there are three kinds of state in the composite structure as shown in Figure 4.26. A-site, polymer intercalated into the interlayer space of clay is weakly bound by Van Der Waals forces and hydrogen bonds to the hydrated interlayer cation and the silicate layer, respectively. B-site, polymer is bound to the clay surface by hydrogen bonds with exchangeable surface cations in the structure of clay. Finally, C-site, a free polymer network is formed between the clay particles. Therefore, the overall structure of the composite would be quite complex. Understanding this complex structure will assist in predicting or searching the composite properties (7).

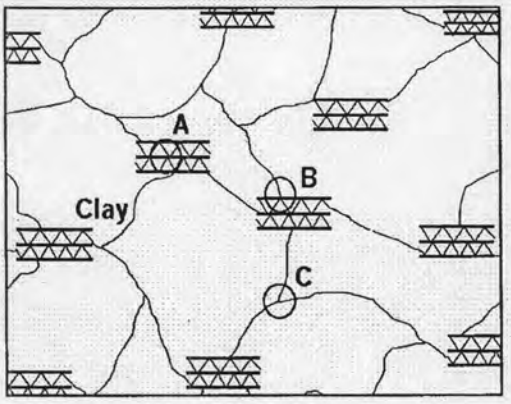

Figure 4.26 schematic structure of a poly(acrylamide)/bentonite composite SAP. A-site: Polymer intercalated into the lamina of bentonite, B-site: Polymer attached to the surface of bentonite particles, C-site: Free polymer network.

4.4.2.2 TEM Analysis

XRD is a conventional method to determine the interlayer spacing of clay layers in the original clay and in the intercalated polymer/clay nanocomposites. On the other hand, the internal structures of the nanocomposites on a nanometer scale are observed using a TEM technique. Such a technique allows a qualitative understanding of the internal structure through direct observation. It was found that poly(AM-*co*-IA)/mica nanocomposites, seen in Figure 4.27, has a partially intercalated structure. Moreover, the TEM micrograph in Figure 4.28 shows the dark cross lines indicating the parts of the intercalation of the polymer in the superabsorbent polymer nanocomposites. On the other hand, the dark lines in the pictures are about 1 nm thick of the clay layers, the space between the dark lines are interlayer spaces, and the gray bases are the polymer matrix. This demonstrates that the organic phase (copolymer) and inorganic phase (the mica particle) are dispersed at the nanometer level. As a result, these nanocomposites exhibit unique properties not being shared by their micro-scale counterparts or conventionally filled polymer (12). However, the

interlayer distances of mica in the nanocomposites from TEM micrograph (Figure 4.28) is about 13.33 Å. This value closes to the value of XRD analysis (Table 4.11). More TEM micrographs of the polymer nanocomposites are illustrated in APPENDIX C.

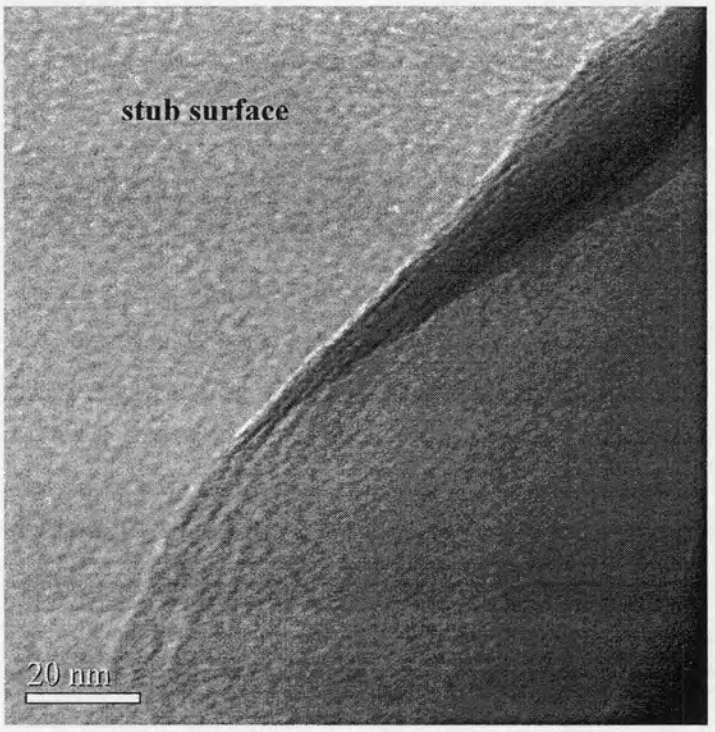

Figure 4.27 TEM micrograph of poly(AM-*co*-IA)/mica nanocomposites, show a partially intercalated structure.

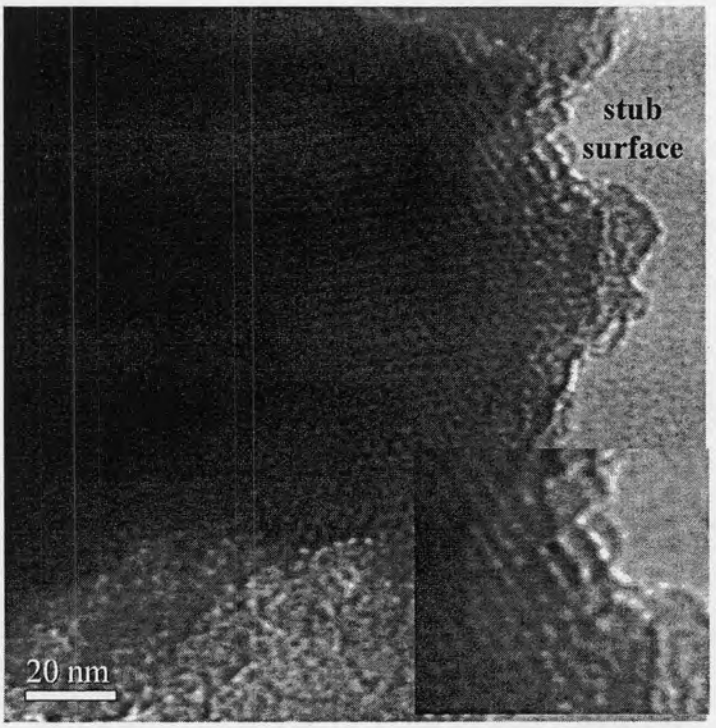

Figure 4.28 TEM micrograph of poly(AM-*co*-IA)/mica nanocomposites.

4.4.2.3 Micro-morphology Analysis

The SEM micrograph of mica particles is shown in Figure 4.29 (a) in which the particle size is approximately 3 μm as shown in APPENDIX B. The surface of copolymer without the mica addition appears to be rather smooth (Figure 4.29 (b)). However, the mica particles were presence and well dispersed in the matrix of the superabsorbent polymer nanocomposite being clearly noted and the mica clusters have the size of about 30-50 μm (Figure 4.29 (c,d)). It is usually observed that the sub-micron sized particles agglomerated themselves to become a loose agglomerate or a tight aggregate imbedded in the polymer matrix.

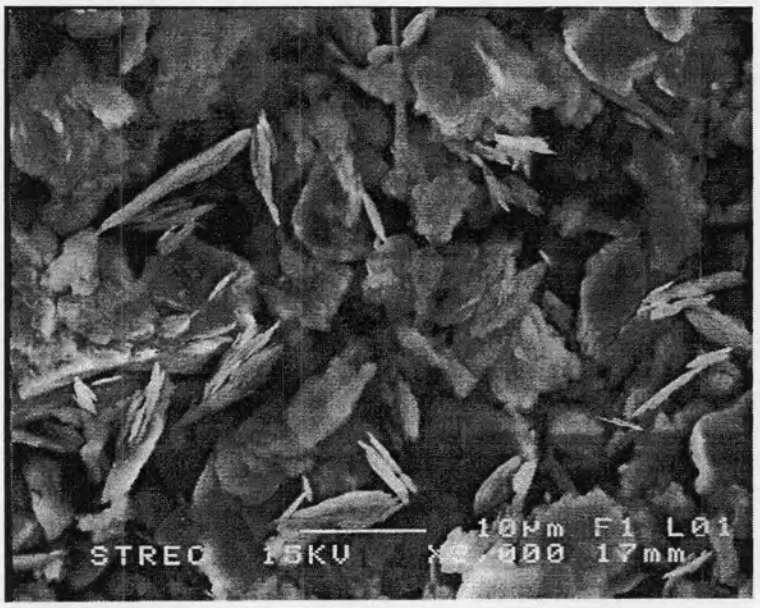
10μm F1 L01
STREC 15KV X2,000 17mm

(a)

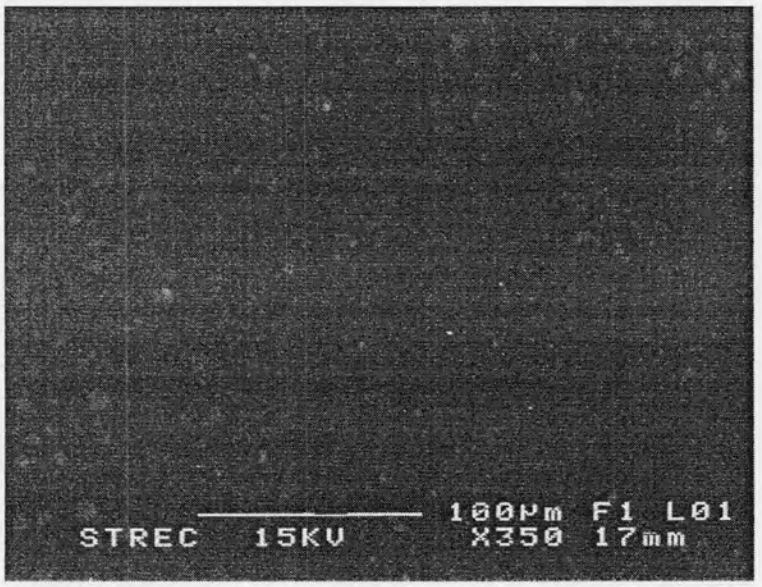
100μm F1 L01
STREC 15KV X350 17mm

(b)

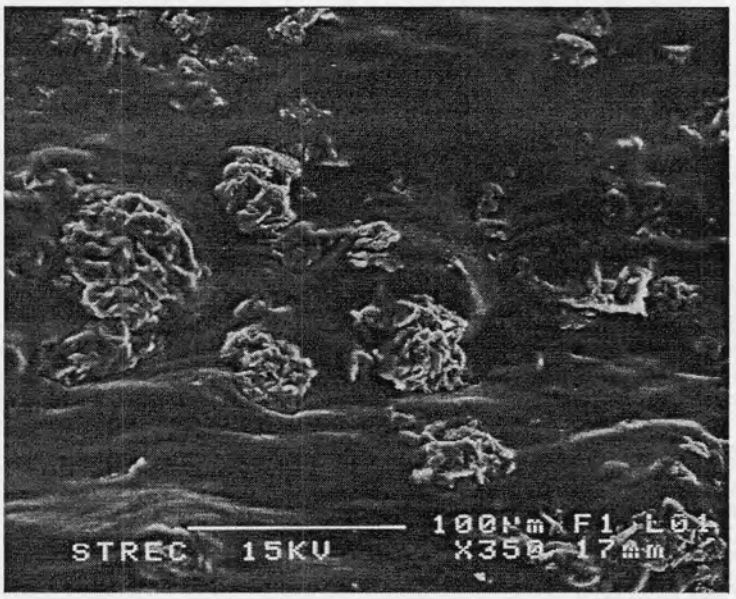

(c)

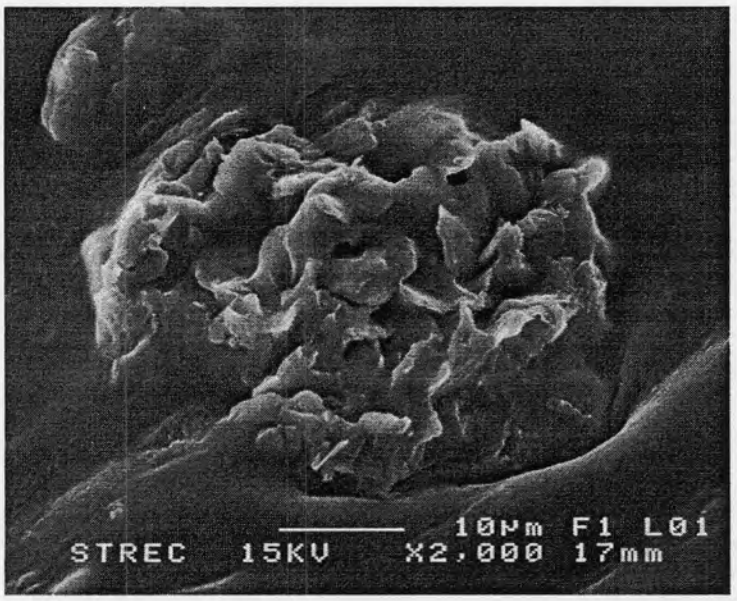

(d)

Figure 4.29 SEM micrographs of (a) mica, (b) mica-free superabsorbent polymer, (c,d) superabsorbent polymer/mica nanocomposites at different magnifications.

4.4.3 Thermal Properties

4.4.3.1 Effect of Itaconic Acid Concentration on the Thermal Properties of Poly(AM-*co*-IA) Copolymer

Thermogravimetric analysis (TGA) was employed to characterize the thermal properties of the synthesized poly(AM-*co*-IA) copolymer as shown in Figure 4.30 and Table 4.12.

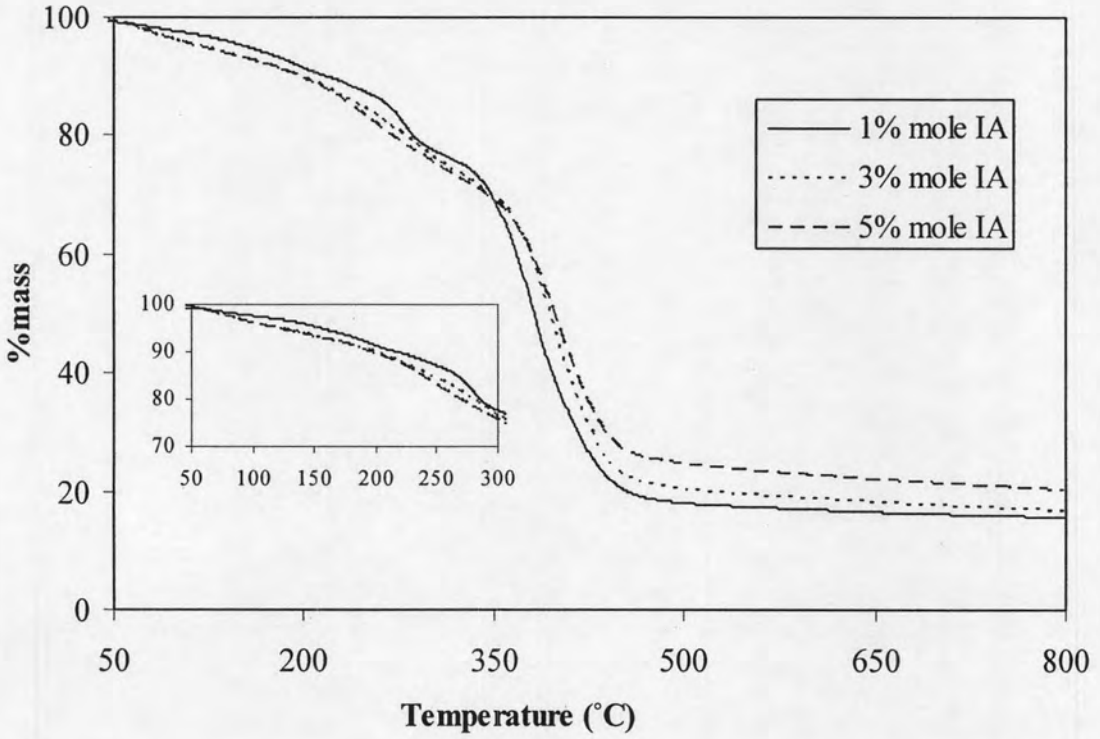

Figure 4.30 TGA thermograms of poly(AM-*co*-IA) copolymer with various IA concentrations at 0.2% mole of N-MBA, 0.3% mole of APS, 1.2% mole of TEMED, 50°C, and 30min.

Table 4.12 Thermogravimetric data of the synthesized poly(AM-*co*-IA) copolymer

IA concentrations (%mole)	Number of decomposition stage	Temperature range (°C)	DTG maxima (°C)	Weight loss (%)	Residue at 800°C
1	1	25-215	195	9.8	15.7
	2	215-310	281	13.5	
	3	310-800	383	60.9	
3	1	25-140	82	6.1	16.8
	2	140-332	290	22.9	
	3	332-800	398	54.3	
5	1	25-210	81	11.4	20.2
	2	210-325	238	16.2	
	3	325-800	400	52.2	

DTG = differential thermal gravimetry

The TGA results as shown in Figure 4.30 and Table 4.12 indicate that the thermal properties of the poly(AM-*co*-IA) copolymer increase with increasing IA concentration. The reason is because of an increase in the intermolecular forces from an increase in the main chain polarity from the addition of IA (40). It is observed that there are three main degradation stages in all formulations. The first stage at 81-195 °C found 6.1-11.4 % weight loss which is due to evaporation of the free water and bound water. The second stage at 238-290 °C found 13.5-22.9 % weight loss according to the decarboxylation of IA coupled with the chain scission. While at 383-400 °C for the final stage of decomposition, a large amount of weight loss (52.2-60.9 %) can be assigned to the degradation of acrylamide portion. This final degradation includes those temperatures higher than 400 °C in which a rapid decomposition to carbon dioxide and volatile hydrocarbons was anticipated (23).

4.4.3.2 Effect of Mica Content on the Thermal Properties of Poly(AM-*co*-IA)/mica Nanocomposites

The effect of mica content on the thermal properties is shown in Figure 4.31. The thermogravimetric data are shown in Appendix D.

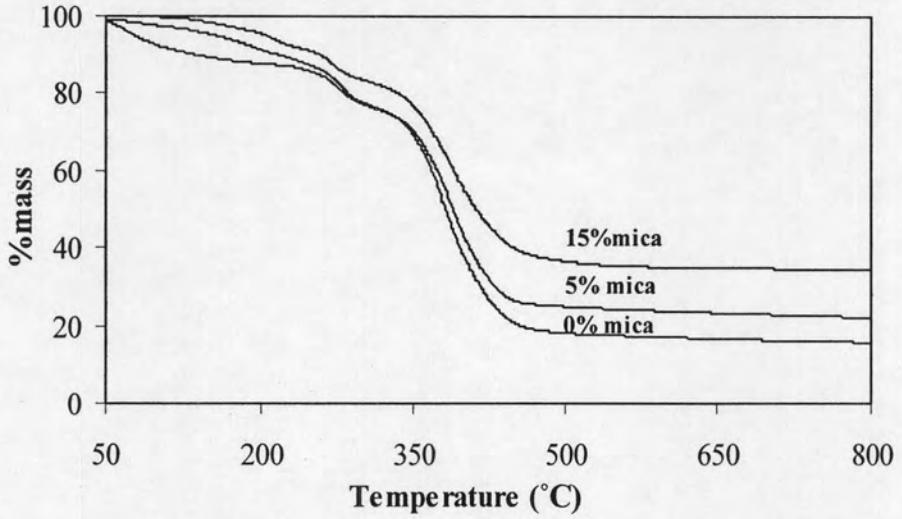

(a)

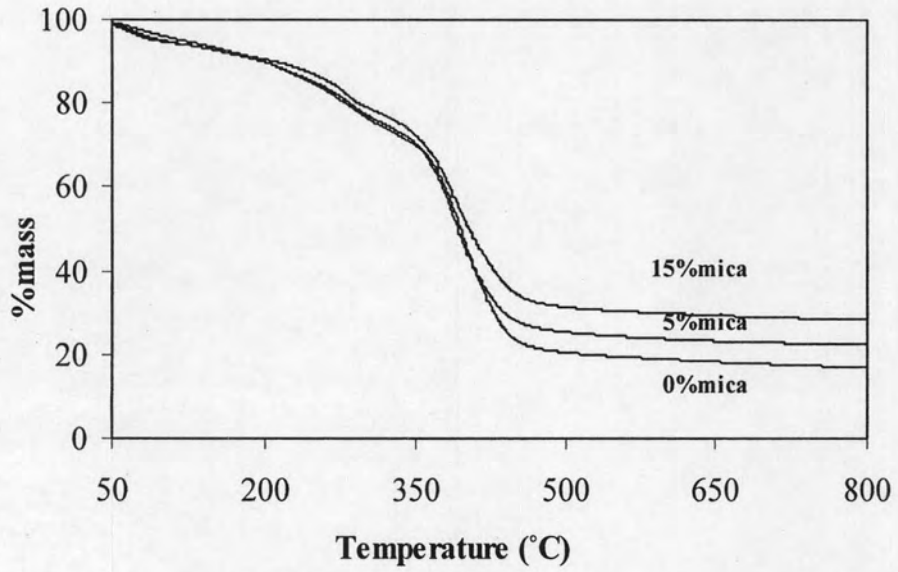

(b)

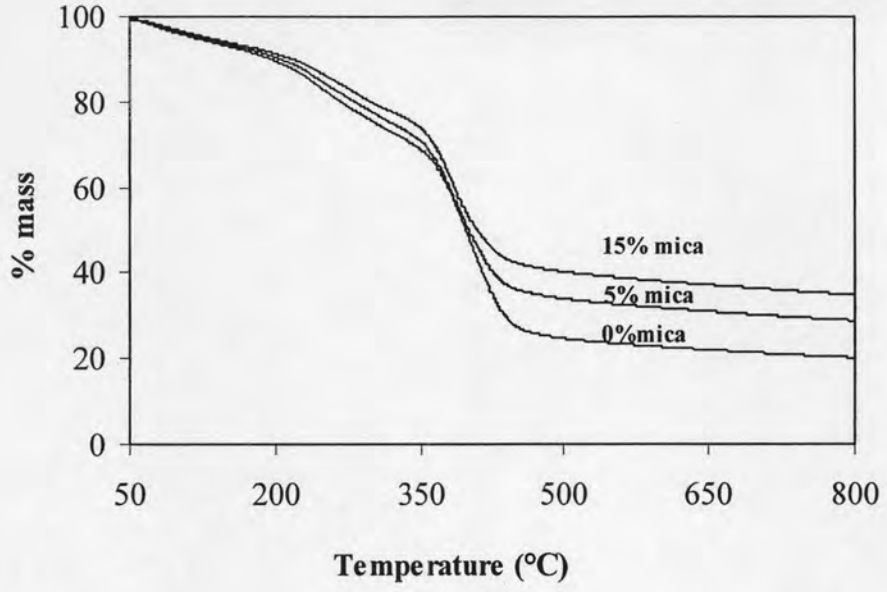

(c)

Figure 4.31 TGA thermograms of poly(AM-*co*-IA)/mica nanocomposites at various mica contents and AM/IA mole ratios for (a) 99/1, (b) 97/3, and (c) 95/5 (with 0.2% mole of N-MBA, 0.3% mole of APS, 1.2% mole of TEMED, 50°C, and 30 min).

The TGA results are shown in Figure 4.31. For poly(AM-*co*-IA)/mica nanocomposites, the thermal stability of mica and residue at 800 °C are both increased with increasing mica content in comparison with the neat poly(AM-*co*-IA) (0% mica). The increases in the thermal stability can be attributed to the high thermal stability of mica and to the interaction between the mica particles and the polymer matrix (4). Moreover, the thermal stability of the composites is enhanced with the increasing mica content from 5 to 15 wt%. This is an additional evidence of mica dispersion in the polymer matrix. Mica acts as a heat barrier, thus delaying the diffusion of volatile thermo-oxidation products to become gas, which results in the enhanced thermal stability of the system (39).

4.5 Swelling Kinetics of the Synthesized Copolymer

The swelling kinetics of the superabsorbent polymers prepared with the AM-to-IA ratio of 99/1 was measured in distilled water in terms of water absorbency as shown in Table 4.13 Figure 4.32.

Table 4.13 Dependence of water absorbency on swelling time of the superabsorbent polymer*

poly(AM-*co*-IA) copolymer		poly(AM-*co*-IA)/mica nanocomposites at			
		5%wt mica		15%wt mica	
Time (min)	Water absorbency (Q) g g^{-1}	Time (min)	Water absorbency (Q) g g^{-1}	Time (min)	Water absorbency (Q) g g^{-1}
1	251±4	1	239±10	1	201±9
5	310±7	5	290±9	5	212±8
10	313±6	10	305±7	10	230±8
30	337±9	30	327±5	30	238±7
60	340±6	60	330±4	60	235±6
180	347±8	180	341±7	180	248±10
300	357±4	300	348±8	300	255±5
480	371±10	480	350±8	480	350±9

*Polymerizations were carried out at the AM/IA ratio of 99/1, 0.2% mole of N-MBA, 0.3% mole of APS, 1.2% mole of TEMED, mica contents at 5 and 15% wt, 50°C, and 30 min.

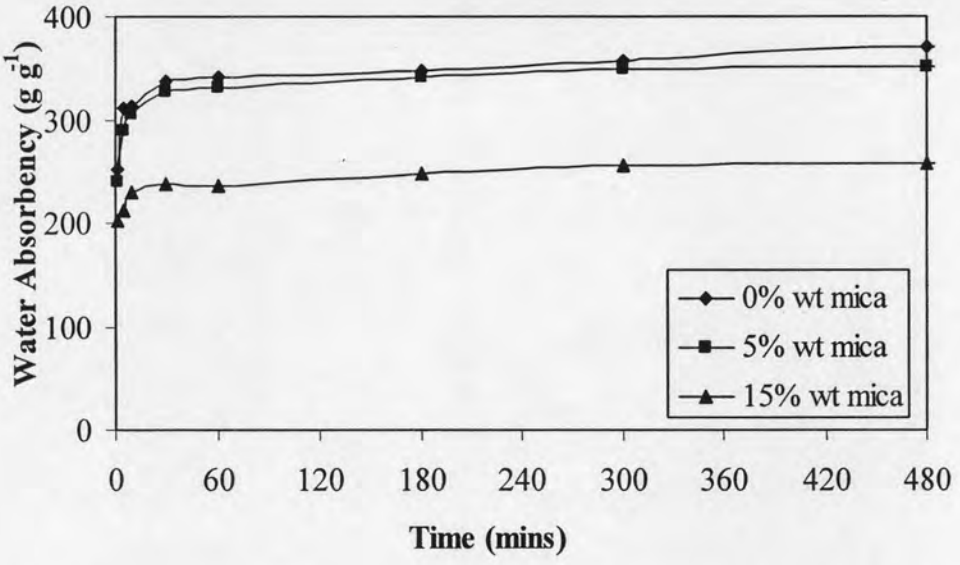

Figure 4.32 Dependence of water absorbency on swelling time of the synthesized superabsorbent polymer nanocomposite having the particle sizes of 150-200 μm prepared by the AM/IA ratio of 99/1, 0.2% mole of N-MBA, 0.3% mole of APS, 1.2% mole of TEMED, mica contents at 5 and 15% wt at 50°C for 30 min.

The synthesized copolymer and poly(AM-*co*-IA)/mica nanocomposites with 0, 5 and 15% wt mica can absorb water up to 251±4, 239±10 and 201±9 g g^{-1} of the dry copolymer within 1 min, respectively. The results shown in Table 4.13 and Figure 4.32 indicate that the more the mica content in the nanocomposites, the lower the absorption rate for poly(AM-*co*-IA)/mica nanocomposites due to the rigidity of the polymer chains resulting from a larger number of the crosslink density of the nanocomposites (5). The absorption rate sharply increased at the beginning, and the equilibrium absorbency could be achieved in 60 min for all of the polymers. After 60 min, the swelling rate was slightly slow down.

4.6 The Mica Incorporated in the Nanocomposite

The amount of retained mica in the nanocomposite, synthesized with the AM/IA ratio of 99/1, 97/3, and 95/5, with 0.2% mole of N-MBA, 0.3% mole of APS, 1.2% mole of TEMED at 50°C for 30 min, is shown in Table 4.14.

Table 4.14 The retained mica in the synthesized poly(AM-*co*-IA) nanocomposites at various mica contents

Mole ratio of AM:IA	(%) mica retained in the composite at various mica contents (%wt)*			
	2	5	10	15
99/1	75	79	79	80
98/2	75	75	75	75
97/3	75	75	75	75
96/4	75	75	75	75
95/5	75	75	75	75

Polymerization was carried out at 0.2% mole of N-MBA, 0.3% mole of APS, 1.2% mole of TEMED, 50°C, and 30min.

The amount of mica retained in the composites was analyzed for 1 g of the superabsorbent polymer composite. The percentages of mica retained in the composites as shown in Table 4.14 are in the range of 75-80 %. It indicates that the larger amount of the mica is indeed intercalated into the polymer network and the

smaller amount of about 20% is distributed in the suspension during the preparation of the superabsorbent.

4.7 Determination of the Unreacted Amounts of Acrylamide Monomer in the Superabsorbents Polymer by Gas Chromatography

The measurement of the unreacted amount of acrylamide monomer after polymerization was important in this research, because acrylamide monomer has been classified as a probably carcinogenic substance in humans. However, polyacrylamide is not considered hazardous for users (41).

The unused amount of acrylamide monomer in the gel after polymerization were characterized by following the METHOD 8032A and the results are shown in Table 4.15 in which the standard curve of brominated sample is shown in APPENDIX A (Figure A-1).

Table 4.15 The residual amounts of acrylamide monomer in the polymer from the solution copolymerization*

AM/IA ratio	Added acrylamide monomer in polymerization reactions (ppm)	Residue of acrylamide monomer in the polymer by weight	
		ppm	%
100/0	7,1080.00	94.2	0.133
99/1	7,0369.20	54.69	0.078
95/5	67,526.00	56.47	0.084

*Polymerizations were carried out at 0.3% mole of APS, 0.2% mole of N-MBA, 1.2% mole of TEMED, 50°C and 30min.

The residual amount of N-MBA from polymerization was considered to be small, since N-MBA was added at only 2% mole, and it can react with other monomer according to its high reactivity ratio. The reactivity r_1 and r_2 values for the system of AM/N-MBA are 0.64 and 1.77 respectively (42). In this case the N-MBA has a small chance to react in the bromination. Therefore, the analyzed value of the residual monomer is obtained mostly from the acrylamide monomer. It is also noticed that the residual amount of the acrylamide monomer retained in the polymer is very minute (approximately 0.1%). These results suggest that the solution polymerization is an acceptable synthesis route to prepare the superabsorbent polymer. Moreover, the solution polymerization method can also be applied to prepare the superabsorbent polymer nanocomposites.

4.8 Determination of Density of the Synthesized Poly(AM-*co*-IA)/mica Nanocomposites

The main application of the synthesized superabsorbent nanocomposites is to produce the personal care product, such as the adult and baby diapers. The desired superabsorbent polymer/composite which does not add the extra load to the diaper will provide comfort to users. Hence, the densities of mica, poly(AM-*co*-IA), and poly(AM-*co*-IA)/mica nanocomposites were investigated. The results are shown in Table 4.16. It was found that the densities of the polymer/mica nanocomposites are increased from 0% to 15% wt of mica, which are approximately 8.76 and 20.44 % of density increment, respectively, compared with that of 0% mica addition. These results indicate that the only 5% mica addition does not increase the density of the superabsorbent polymer too much. Such addition has a trivial effect on the total

weight of superabsorbent polymer. Moreover, 5% mica addition also provides the superabsorbent polymer nanocomposites with the highest water absorbency.

Table 4.16 The densities of mica, poly(AM-*co*-IA), and poly(AM-*co*-IA)/mica nanocomposites *

Superabsorbent Polymer Poly(AM-*co*-IA), %w/w	Mica Content Added, %w/w	Density (g cm^{-3})
-	100	1.94±0.03
100	0	1.37±0.04
100	5	1.49±0.01
100	15	1.65±0.03

*Polymerizations were carried out at AM/IA ratio of 95/5, 0.2% mole of N-MBA, 0.3% mole of APS, 1.2% mole of TEMED, 50°C, and 30 min.